*Manuscript
Click here to view linked References

Streamlined islands and the English Channel megaflood hypothesis

J.S. Collier [1†], F. Oggioni [1*], S. Gupta [1], D. Garcia-Moreno [2,3], A. Trentesaux [4], M. De Batist [3]

1 Dept. Earth Science & Engineering, Imperial College London, Prince Consort Road, SW7 2BP, UK.
2 Royal Observatory of Belgium, Av. Circulaire 3, 1180 Uccle, Brussels, Belgium.
3 Renard Centre of Marine Geology, Ghent University, Krijgslaan 281 S.8, B-9000 Ghent, Belgium.
4 Université de Lille, UMR CNRS 8187 LOG, 59 655 Villeneuve d'Ascq, France.

† Corresponding author: jenny.collier@imperial.ac.uk
* Now at CGGVeritas Services, Crompton Way, Manor Royal Estate, Crawley RH10 9QN, UK

Keywords:
Streamlined islands; Catastrophic flooding; North-west European glaciations

Abstract

Recognising ice-age catastrophic megafloods is important because they had significant impact on large-scale drainage evolution and patterns of water and sediment movement to the oceans, and likely induced very rapid, short-term effects on climate. It has been previously proposed that a drainage system on the floor of the English Channel was initiated by catastrophic flooding in the Pleistocene but this suggestion has remained controversial. Here we examine this hypothesis through an analysis of key landform features. We use a new compilation of multi- and single-beam bathymetry together with sub-bottom profiler data to establish the internal structure, planform geometry and hence origin of a set of 36 mid-channel islands. Whilst there is evidence of modern-day surficial sediment processes, the majority of the islands can be clearly demonstrated to be formed of bedrock, and are hence erosional remnants rather than depositional features. The islands display classic lemniscate or tear-drop outlines, with elongated tips pointing downstream, typical of streamlined islands formed during high-magnitude water flow. The length-to-width

ratio for the entire island population is 3.4 ± 1.3 and the degree-of-elongation or k-value is 3.7 ± 1.4. These values are comparable to streamlined islands in other proven Pleistocene catastrophic flood terrains and are distinctly different to values found in modern-day rivers. The island geometries show a correlation with bedrock type: with those carved from Upper Cretaceous chalk having larger length-to-width ratios (3.2 ± 1.3) than those carved into more mixed Paleogene terrigenous sandstones, siltstones and mudstones (3.0 ± 1.5). We attribute these differences to the former rock unit having a lower skin friction which allowed longer island growth to achieve minimum drag. The Paleogene islands, although less numerous than the Chalk islands, also assume more perfect lemniscate shapes. These lithologies therefore reached island equilibrium shape more quickly but were also susceptible to total erosion. Our observations support the hypothesis that the islands were initially carved by high-water volume flows via a unique catastrophic drainage of a pro-glacial lake in the southern North Sea at the Dover Strait rather than by fluvial erosion throughout the Pleistocene.

1 Introduction

1.1 The Channel River

The floor of the English Channel (La Manche), the seaway between England and France, is characterised by a network of sediment-filled and unfilled palaeochannels, which are generally referred to as the Channel River (Fleuve Manche, Figure 1). The system can be traced from the Dover Strait (Pas de Calais) at the southern limit of the North Sea to a Neogene tectonic lineament known as the Hurd Deep (Hamilton and Smith 1972; Lericolais et al., 1995; Lericolais et al., 1996). In turn, the Hurd Deep connects to the Western Approaches and finally to the shelf-break in the Bay of Biscay (Lericolais et al., 2003). The Western Approaches also host a network of palaeovalleys but it is not possible to directly correlate them to those in the Eastern English Channel (Le Roy et al., 2011). However, it is widely inferred that the Channel River flowed across this whole zone during Pleistocene sea-level low-stands to supply sediments to the deep sea fans in the Bay of Biscay (Bourillet et al., 2003; Toucanne et al., 2009). The Channel River is therefore a key

element of the British/Scandinavian ice-sheet system, especially when they coalesced across the northern North Sea during the Anglian-Elsterian (~450 ka, MIS12 or ~350 ka, MIS10) and late Saalian (~160 ka, MIS6) glaciations, making it the main discharge route for the major NW European rivers to the Atlantic (Gibbard, 1988). Here we present an analysis of a key geomorphic element of the unfilled palaeochannels in the eastern English Channel between the Dover Strait and the Hurd Deep in order to gain insights into the development of the Channel River system as a whole.

A critical element in understanding the development of the Channel River is the opening of the Dover Strait. There is a consensus that for much of the Pleistocene the landmasses of England and France were connected via the northern limb of the Weald-Artois anticline, such that the North Sea and English Channel were separate seaways even during sea-level high-stands (Gibbard, 1995; Meijer and Preece, 1995; Van Vliet-Lanoe et al., 1998). How and when this barrier was removed however is disputed. Of the various ideas proposed over the years, two potential models remain under discussion today. The first model suggests that the Channel River formed incrementally during the glacial cycles, with a slow erosion of the rock barrier at the Dover Strait by fluvial action during low-stands and tidal scour during high-stands (Dingwall, 1975; Westaway and Bridgland, 2010; Hijma et al., 2012; Mellett et al., 2012; Mellett et al., 2013). This model assumes there was no involvement in removal of the Dover Strait barrier of a pro-glacial lake in the southern North Sea that formed when the British and Scandinavian ice sheets met across the northern North Sea and so blocked northward drainage of both glacial meltwater and fluvial discharges from European rivers such as the Rhine/Meuse. The second model suggests that the Channel River was initially carved by catastrophic breaching of the Weald-Artois structure and catastrophic drainage of the pro-glacial lake (Smith, 1985; Gibbard, 1995; Gupta et al., 2007; Cohen et al., 2014; Gibbard and Cohen, 2015; Figure 1 inset). According to this model the Channel River was initially carved by an extra-ordinary release of water from an overspill at the Dover Strait but subsequently carried more typical glacial-retreat fluvial discharges down it. The key in discriminating between the models is not therefore recognising “normal” pro-glacial surface processes, but rather recognising features that could have only originated from anomalously high

79 water discharges (Baynes et al., 2015). It is important to establish how the Channel River formed as it
80 undoubtedly took a major role in the palaeo-geographic evolution of NW Europe and there are potentially
81 significant palaeo-climate implications if the delivery of a large pulse of fresh water due to breaching was
82 sufficient to destabilise the North Atlantic thermohaline circulation.

83 *1.2 Recognising pro-glacial megafloods*

84 It is now well-established that the Pleistocene deglaciations involved huge fluxes of water from the wasting
85 continental ice sheets, and that much of this water was delivered as floods of immense magnitude and
86 relatively short duration (Marshall and Clarke, 1999). Since the pioneering work in the Channeled Scabland
87 region (Bretz, 1923, Baker and Nummedal, 1978) pro-glacial megaflood scoured landscapes are now
88 recognized in many other areas of North America, including near the Great Lakes and adjacent St. Lawrence
89 Basin (Kehew, 1993); the Hudson River Basin (Kor et al., 1991); the Mackenzie River Basin (Murton et al.,
90 2010); the Yukon Basin (Clarke and Mathews, 1981) and the Alaskan Susitna, Tok, and Copper River Basins
91 (Wiedmer et al., 2010). In Eurasia, Pleistocene megaflood outbursts have been reported in the German
92 Weser Valley (Meinsen et al., 2011), from the Baltic Ice Lake in Sweden (Elfstrom and Rossbacher, 1985)
93 and along the Siberian Yenesei River and Ob River in the Altai Mountains (Komatsu et al., 2009; Rudoy,
94 2002). Megaflooding is therefore a known behaviour of all well-studied continental ice-sheets, and we draw
95 on these previous studies, together with those from fluvial and tidal settings, to interpret our English
96 Channel observations.

97 Studies of pro-glacial outburst floods from the locations detailed above together with those from Holocene
98 and modern glacial-lakes have established two types of criteria for their recognition: one based on palaeo-
99 hydraulic reconstructions and one based on the assemblage of erosional and depositional features
100 produced. In the former group the most common approach is to estimate the peak rate of water discharge
101 from the channel geometry. Values for well-established Pleistocene megaflood terrains range between 0.6
102 and 18 Sv (1 Sv being $x10^6$ m^3/s, from where the prefix “mega” originates, e.g., O'Connor and Baker, 1992;

O'Connor, 1993; Rudoy, 2002; Clarke et al., 2004; Komatsu et al., 2009). These peak flow rates are 1 or 2 orders of magnitude greater than those generated by modern-day rivers, Pleistocene rivers or overspill from Holocene glacial-bound lakes (e.g., Cenderelli and Wohl, 2001; Rudoy, 2002; Carrivick et al., 2004; Alho et al., 2005). In the Channel River case the peak discharge rate has been estimated to be between 0.5-1.0 Sv (Gupta et al., 2007; Westaway and Bridgland, 2010) making it comparable to previously documented Pleistocene megaflood examples.

In terms of the second approach to recognising Pleistocene megafloods, past studies have documented specific geomorphic assemblages associated with such high magnitude discharges (Baker, 1978; Kozlowski et al., 2005; Lamb et al., 2014). At spillpoints the landscape is characterised by cataracts, plunge pools and linear striations. In distal parts diagnostic indicators include: (i) a deep, wide, steep walled channel morphology; (ii) scour zones and erosional terraces; (iii) hanging valley tributaries; (iv) streamlined erosional residuals; (v) the presence of large-scale bars; (vi) inversely graded boulder-gravels; and (vii) coarse-grained fan deposits where channels terminate. In the case of the English Channel the region was repeatedly exposed and transgressed during late Quaternary sea-level fluctuations and is today submarine. This clearly makes its study more difficult than the flood-terrain examples within the continental landmasses of North America and Eurasia, and limits discussion to erosional features alone. On the other hand there is no evidence for any Quaternary ice sheets having covered the study area at any point (Ehlers et al., 2011), thus removing any possibility of the influence of sub-glacial processes. In our earlier work we presented the first evidence for catastrophic flood-generated landforms from a small region of the Channel River system (Figure 3a, Gupta et al., 2007). Here we extend this analysis for the entire system, apply sub-bottom constraints and undertake a detailed analysis of the mid-channel islands.

1.3 Streamlined islands

Islands are present in nearly all major river systems on Earth (Gurnell and Petts, 2002) and often possess a tear-drop plan-view shape, with the tip pointing downstream. Owing to their similarity to symmetrical

127 airfoils, such islands are generally referred to as “streamlined islands”. Mathematically, the shape is
128 equivalent to a half lemniscate loop according to the relation $r=L\cos(k\theta)$, where r and θ are polar co-
129 ordinates, L is island length and k is the elongation factor (see section 2.3; Komar, 1983). Field examples
130 show that the distinctive streamlined island shape can either be built through fluvial deposition or be the
131 result of removal of the material around them (hereafter referred to as “depositional islands” and
132 “erosional remnant islands” respectively). Both island types have been simulated in flume experiments with
133 the various forms being generated under different flow conditions (Komar, 1983). Of course, in reality
134 islands in river channels are often formed by a dynamic response to the interplay of both factors, but here
135 we are referring to the *dominant* process.
136
137 Depositional islands can be built by several processes some of which are related to “normal” (as opposed to
138 mega-) flood related (such as avulsion and lateral shifts in channel position) and others which are not (such
139 as sediment deposition in the lee of an obstacle, Osterkamp, 1998; Wyrick and Klingeman, 2011;
140 Moscardelli and Wood, 2011). In some cases, erosional remnant islands can have partial accretion behind
141 them, such as is seen in the Channeled Scablands (where they are referred to as “pendant bars”; Baker,
142 2009a). However islands formed entirely by accretion are generally produced in braided river systems
143 under sustained, moderate flows over moderate-to-low gradient reaches (Wyrick, 2005; Tooth and
144 McCarthy, 2004). Depositional islands are inherently unstable as the channels surrounding them tend to
145 laterally migrate. Several studied have highlighted the importance of vegetation in their development and
146 evolution (e.g. Detriche et al., 2010). Modern-day periglacial environments most commonly host braided
147 rivers with unstable depositional islands (Vandenberghe, 2001) and these are thought to have also
148 characterised Pleistocene glacial rivers (Vandenberghe, 2002).

149 Erosional remnant islands are found in modern-day rivers in tectonically uplifting regions such as Africa and
150 India which are characterised by high gradients where long-term transport capacity exceeds sediment
151 supply (Kale et al., 1996; Tooth and McCarthy, 2004 and references therein). These rivers are generally

termed “anabranching” to distinguish them from braided rivers with depositional islands and are much rarer (Tooth and Nanson, 2000; Vandenberghe, 2001). In modern examples, the gradient seems to be the most critical parameter for island formation. For example along the Orange River of southern Africa, a change from depositional to erosional island formation occurs when the gradient steepens above 0.0013 (Tooth and McCarthy, 2004). This threshold is a factor of 10 times steeper than the channel floor gradient anywhere in our study area. Some studies have also highlighted suitable bedrock as a secondary requirement for eroded island formation today. An alternative setting in which to generate erosional remnant islands is by extreme water flows. Indeed, erosional remnant islands are one of the primary forms of evidence for extreme floods that totally overwhelm an existing drainage network (Kehew and Lord, 1986). Initially, such flows develop a multi-branched channel pattern controlled by pre-existing irregularities of the surface topography. These irregularities act as obstacles to the flow path and cause it to divide and then re-join downstream of them. Erosional modification by the flow, given a sufficient amount of time, will cause the obstacle to develop a streamlined shape. Baker, 1978 was the first to propose that under these conditions, the streamlined island shape represents an equilibrium geometry for a given water flow regime produced in order to minimise total drag by balancing the skin friction across their surface and the pressure drag developed by the turbulent wake behind them. The pressure drag is reduced by elongation of the island but only to the point where there is a trade-off against increased skin friction due to the larger surface area. Flume experiments suggest that this reshaping of the obstacles is most efficient when the waters fully submerge them such that the flow across the island top becomes supercritical (Komar, 1983), however these processes have not been explored in detail.

1.4 Study aims

In this paper we use a new compilation of marine geophysical datasets to produce the first detailed map of the unfilled portions of the Channel River between the Dover Strait and Hurd Deep and characterise the morphology of a set of mid-channel islands. The study will focus on two main areas, previously named as the Northern Palaeovalley and Lobourg Channel (Smith, 1985, figure 2). Using both seabed and sub-seabed

imagery, we: (i) describe the island population and their relationship to the channel, (ii) demonstrate that the islands are bedrock remnants rather than depositional features, (iii) establish that the islands do indeed conform to a lemniscate planform geometry expected for streamlined islands, (iv) show how island shape correlates with geological bedrock type, and (v) show that the channel morphology and streamlined island population compares directly to those found in other known Pleistocene megaflood terrains. Based on these findings we propose that the islands further support the hypothesis that the English Channel experienced a catastrophic flood, consistent with an overspill event of a pro-glacial lake. Finally we will present evidence from channel tributaries which further support this conclusion.

2 Methods

2.1 Bathymetric data acquisition and processing

We have compiled a suite of bathymetric and sub-bottom datasets from a range of sources across the study area (Figure 2). The bathymetry data includes single-beam echo soundings from the UK and French government hydrographic services (UKHO and SHOM respectively) which were combined with swath bathymetry data collected between 2003-2012 by the UK Maritime and Coastguard Agency (MCA), the Marine Aggregate Levy Sustainability Fund (MALSF) and the Royal Observatory of Belgium and the Renard Centre of Marine Geology, Ghent University (ROB-RCMG). Where we were unable to source sufficient soundings ourselves we infilled with the 30 arc-second (~900 m cell size) GEBCO grid, which in the study area contains significant single-beam echo soundings from fishing vessels via Olex-AS (GEBCO, 2008). Prior to merging the soundings from the various sources, a number of small (<2 m) depth bulk-shifts were made to individual datasets to correct them to the UK Ordnance Datum. All positions were also converted into UTM zone 31. A single grid of the entire study area was then produced with a cell size of 30 m using IVS DMAGIC. Separate grids of areas covered by the swath bathymetry (MBES) data were made with cell sizes between 1.5-7 m depending on data quality/density. Further details are given in Oggioni, 2013 and García-Moreno et al., 2015. To help the interpretation of the surfical sediment cover by understanding the

modern-day hydrodynamics we also made use of a model of the predicted seabed shear stress resulting from the modern-day tidal currents (Mitchell et al., 2010; Figure 3d). This is a fully hydrodynamic, non-hydrostatic, finite element model that solves the Navier–Stokes equations on an unstructured finite element mesh. The model has been validated extensively against real-world tidal datasets.

2.2 Sub-bottom seismic data acquisition and processing

The digital sub-bottom data used here come from four individual surveys conducted between 2003 and 2010 under the UK MALSF (Gupta et al., 2004; James et al., 2007; James et al., 2010; James et al., 2011; Figure 2). All were collected with boomer/sparker sources and single-channel streamers, except the Arun dataset which used a multichannel streamer (Gupta et al., 2004). The dominant frequency content of the data is 1-5 kHz, giving a penetration of up to 50 m and a vertical resolution of 0.2-0.4 m. Shot spacings vary due to strong tides making it difficult to maintain vessel speed, but are typically between 1 and 3m. As both the source and receivers were surface towed, there is variable data quality depending on sea-state conditions. Luckily most of the surveys were collected as sets of three closely spaced corridor lines, so the best of the three could be used. Where needed, post-acquisition data processing such as band-pass filtering, swell-filtering, tidal-corrections and time migration were conducted using ProMax software. The processed SEG-Y data were then loaded into a Kingdom Suite project together with the bathymetric grids for interpretation.

2.3 Interpretation

The gridded bathymetric data were analysed within IVS Fledermaus v7.4 (to provide illuminated renditions of the DEM) and Arc-GIS v10.2 (for all the actual mapping). First the main components of the unfilled channel were manually mapped and mid-channel islands identified. Any topographically raised feature in a mid-channel position was classed as an island, with no screening for likely streamlined forms. The island outlines were then traced using computed bathymetric contours and local slope as a guide (Figure 4a,b).

Within the study area the Channel River palaeovalley system crosses the sub-crop geology of five sedimentary basins – the London Basin in the north-east which exposes mainly Tertiary rocks, the Weald-Artois Basin which exposes Jurassic and Cretaceous rocks, the Hampshire-Dieppe Basin which exposes Paleogene rocks, the Channel Basin which exposes Jurassic and Cretaceous rocks and the Central Channel Basin in the south-west which exposes Jurassic to Paleogene age rocks (Hamblin et al., 1992; Figure 3c). These basins were inverted during Miocene Alpine tectonics which produced numerous fold and fault structures. Table 1 summarises the stratigraphy exposed at the seabed across the study area. The lithologies are highly variable with three main types in terms of their resistance to erosion: firstly there are the massively bedded Upper Cretaceous Chalk units; secondly more finely bedded, mixed terrigenous and calcareous units of Paleogene (e.g Barton and Bracklesham Beds), Lower Cretaceous (Greensand and Hastings Beds) and Upper Jurassic (Purbeck, Portland and Kimmeridge Clay) age and thirdly more homogeneous mudstone intervals (Weald and London Clay). The various geological units, and many of the associated geological structures, can be readily identified offshore from bathymetric texture (Collier et al., 2006; García-Moreno et al., 2015). These textures were ground truthed by available cores and digital maps from the British Geological Survey (BGS, made available under the Open Government Licence, © NERC, 2015) and the Bureau de Recherches Géologiques et Minières (BRGM). The major boundaries between the various bedrock units were mapped and the surrounding bedrock geology type was then added to individual island inventories. Note that in some areas offshore the stratigraphic sub-groups are undifferentiated. The bedrock assignment was therefore made to the smallest lithological unit possible. Finally the island shapefiles were imported into the Kingdom Suite project for reference during the interpretation of the sub-bottom seismic data.

To analyse the plan-view island shapes we followed the methods developed in Komar, 1983 and Komar, 1984. He introduced three dimensionless parameters to describe the form: the length-to-width ratio (L/W); the "elongation factor" ($k = (\pi * L^2)/(4A)$, where A=planform area) and the location of its maximum width or "shape factor" (Xm). First we extracted the plan-view areas (A) for the various interpreted island polygons

using built-in functions of Arc-GIS. Each island polygon was then extracted and a first-estimate of its length (using the most upstream and most downstream points) made. These values were then used to calculate the starting k-value (Figure 4c) from which the corresponding lemniscate was calculated using the relation $r=L\cos(k\theta)$, where r and θ are polar co-ordinates. A normalised misfit difference between the computed lemniscate to the actual island polygon was then calculated (Figure 4d). Finally, in order to find the best-fitting lemniscate the island was allowed to rotate by up to 10^0, such that the maximum measured length did not lie along the y=0 axis. The final minimised misfit therefore gives an indication of departure from a perfect lemniscate or streamlined geometry. In practice misfits less than 30% were taken as excellent lemniscate geometries. Finally the shape factor (Xm) was extracted from the point of intersection between the axes of maximum length and maximum width (Figure 4c).

3 Results

3.1 Channel morphology

Our new bathymetric map of the eastern English Channel and interpretation of the unfilled portions of the Channel River are shown in Figure 3. The river channel morphology visible on the Channel floor today is almost certainly the consequence of redistribution of sediment that must have happened since the channels were last occupied. Whether this happened during the marine transgression at the beginning of the Holocene or afterwards is unknown. However, we note there is a strong correlation between the best-swept/ most-sedimented stretches of the system and the predicted seabed shear stress resulting from the modern-day tidal currents (Mitchell et al., 2010; Figure 3d). The palaeochannel system is cleanest where the seabed shear stress is high, and it becomes increasingly choked with sediments where the seabed shear stress reduces. On a smaller scale, there is also a direct correlation between the tidal model predictions and the surficial sediment bedforms, with low seabed shear stress correlating with the presence of kilometre-scale sandbanks (e.g. Figure 6a) and intermediate seabed shear stress and metre-scale sandwaves (e.g. Figure 5c). The modern tides therefore provide an explanation for the overall landscape – in that they

appear to have swept the region free of significant sediment in all but the central part of the study area. This allows morphologic elements on a decimetre-scale to be readily observed. The map shows, for the first time, a clear the linkage of the Northern Palaeovalley with the Lobourg Channel south of the Dover Strait establishing them to be part of the same system. In plan-view the Lobourg Channel - Northern Palaeovalley system traces a broad "S" shape across the study area. The new data compilation also shows a small part of the confluence between the Northern and Southern Palaeovalleys at the eastern tip of the Hurd Deep. However, as the rest of this system is buried and outside of the area where we have new sub-bottom data (Figure 2) we will not discuss this feature further.

We present a set of bathymetric profiles across the Lobourg Channel and Northern Palaeovalley systems in Figure 3b. These show the main channel to typically display an approximately box-shaped cross-sectional geometry. The channel margins are marked with black arrows, and have slopes ranging between 1.5-2.5^{0}. Nowhere do we see any evidence in the sub-bottom data for these margins being directly constrained by geological structures such as faults. Overall whilst the channel widens downstream, being around 9 km wide in the north-east (Profile A) and 13 km wide in the south-west (Profile H) of the study area this does not happen systematically. Rather it widens and then narrows at different points. Similarly, whilst channel depth (vertical distance between the channel flank and floor) ranges between 15 and 30 m, it does so without a clear systematic trend along profile.

Cross-sectional symmetry is seen throughout much of the length of the system, with the outer banks having the same depth e.g., Profile B, D and I. However, mild asymmetry occurs where the system changes azimuth. Here the bank on the outer side of plan-view bend tends to be slightly higher, for example on the UK side in Profile E. In some sections there is an outer channel margin (marked with red arrows) and an intervening terrace. This is widest and best developed in the region of Profile G, but it is also seen on Profile A and F.

There is abundant evidence in our new data compilation for both the Lobourg Channel and Northern Palaeovalley being carved into bedrock as opposed to Quaternary sediment. This is a critical observation for determining their origin. In many places bedrock ridges can be traced from one bank, across the channel floor to the other bank (e.g., Figures 6a, 7c). Overall the channel cross-sectional geometry does not appear to be correlated with bedrock type.

In plan-view the changes in channel azimuth strongly correlate with the bedrock geology (Figure 3c). Major bends in channel planform occur where it: (1) crosses the southern Chalk limb of the Weald-Artois anticline onto the Paleogene rocks of the Hampshire-Dieppe Basin (bearing change of 110^0), (2) where it crosses the Mid Channel Fault that separates the Channel and Central Channel Basins (bearing change of 80^0) and (3) where it joins the Hurd Deep lineament (bearing change of 90^0, Figure 3c). Other geological boundaries correlate with more subtle changes in the channel morphology, for example it undergoes a necking of around 3 km as it crosses from Paleogene to Chalk strata across the Wight-Bray Fault that separates the Hampshire-Dieppe and Channel Basins (Figure 5b). Close to this fault seismic data show the rock units to be near-vertical (Collier et al., 2006), and the most likely explanation for the channel geometry observed is that resistant beds restricted channel widening.

3.2 Island morphology

A total of 36 mid-channel islands were identified (coloured black in Figure 3c). Islands are observed throughout the study area, from the Dover Strait to the point where the system enters the Hurd Deep. Four of the identified islands lie within the Lobourg Channel where they have characteristics that are indistinguishable from those identified elsewhere in the Northern Palaeovalley. For ease of reference the islands are numbered from 1 (east) to 36 (west).

In cross-section, the island margins vary according to bedrock type. Those islands found within the Chalk bedrock consistently present the steepest edges – both in the across- (Profiles A, D, and G, Figure 3b) and along-channel directions (Figure 5c). The islands found within other bedrock units present more varied

forms. Those found within the Jurassic are typically also prominent (Profiles B, C and D (island 13)) whilst those in the Wealden are the least well defined (Profile H). Excluding examples where islands host modern sandwaves, the tops of the islands are generally flat. Some of the islands rise to a height at or slightly below that of the neighbouring channel flanks (e.g., Profiles C, D, G and I); whereas others lie some distance below (e.g., Profiles A, B and H). Some of the taller islands show shallow benches, particularly on their upstream margins e.g., Island 4, Figure 6a. The heights of these benches are consistent with those of the tops of many other islands. One of the islands (Island 25) shows strongly eroded flanks with a narrow and more elevated central part that represents what is left of a formerly larger island (Figure 5b). However, this is unusual as most islands show little evidence for later erosion.

In plan-view, the majority of the identified mid-channel islands have the classic tear-drop shape, with the long axis pointing downstream (e.g., Islands 20-23, Figure 4), but some are more elongate (e.g., Island 24, Figure 4) or lenticular (e.g., Island 30, Figure 5b). Island planform metrics are summarised in Table 2. Island lengths range between 1.5 and 20 km and widths 0.6 to 10 km, with the length-to-width ratio (L/W) for the entire island population being 3.4 ± 1.3. There is no apparent spatial distribution according to size, with large and small islands found adjacent to each other throughout. The islands are generally symmetrical, with little evidence for any of their shapes being controlled by the proximity to either channel bank. Individual islands are typically surrounded by ~1-2 m deep, 200-500 m wide and 8-15 km long scours into the channel floor (Figure 5). These scours are generally sub-parallel to the channel margins but curve around the islands, suggesting they are flow streamlines.

Many of the islands support cross-over channels, which are approximately linear features a few metres deep that cut right-across a given island (e.g., Island 8, Figure 5c). These cross-over channels always occur towards the downstream end of a given island and cut at an oblique angle to the direction of elongation. There are two examples, both on Chalk bedrock, where these cross-over channels have developed into divide crossings which appear to have separated smaller downstream fragments from a previously larger

344 island (Islands 28-27-26, Figure 5b and Islands 18-17-8, Figure 5c). Importantly, as shown most clearly in
345 Figure 5c, the divide crossings are parallel to each other and to the cross-over channel on top of the
346 "mother" island surface. This suggests that the direction of the flows that carved these features remained
347 constant and the process of island development was on-going. Several islands show dendritic, secondary
348 drainage channels superimposed on their tops similar to those seen where the channel has a terrace (e.g.,
349 Island 26, Figure 5b). These features suggest post island formation subaerial exposure and erosion of
350 dendritic drainages by rainfall.

351 ### *3.3 Island distribution*

352 While a few islands are isolated in position, most lie within one of four spatial groups (Group 1: Islands 2-4;
353 Group 2: Islands 5-18; Group 3: Islands 20-31 and Group 4: Islands 32-36). For ease of reference the groups
354 are given different colours in Figure 3d. The break between Groups 1 and 2 may be artificial due to this area
355 having the highest concentration of recent sediments which may completely bury some islands. The break
356 between Groups 2 and 3 however is distinct as there is relatively little surficial sediment and clear bedrock
357 structure visible on the intervening channel floor. This break in islands occurs within Paleogene rocks of the
358 Hampshire Basin. The Paleogene succession here forms a broad syncline, and the island gap corresponds to
359 where the Barton Beds outcrops at the seabed. This unit contains more mudrocks and fewer coarse
360 terrigenous and calcareous beds compared to the older units that outcrop either side (Table 1). So either
361 islands were formed in this softer, less resistant material but were later eroded away or no islands were
362 formed here because the seabed bedrock was more homogeneous, and did not present irregularities
363 needed to initiate the streamlined forms. In either case there appears to be a correlation between the
364 presence today of streamlined islands and bedrock. Indeed the majority of islands (19 out of 36) are found
365 in Upper Cretaceous Chalk bedrock despite this forming just 40% of the seabed along the total reach
366 studied.

The spatial gap between Groups 3 and 4 is the smallest seen and may be perceived because there is a change in island shape. The islands in Group 4 are unlike any of the others seen further upstream, with much lower length-to-width ratios (Table 2). Their shapes may have been influenced by a change in flow dynamics and erosional evolution as the flood flow changed direction as it entered the Hurd Deep.

3.4 Island internal structure

The internal structure of the islands is a critical characteristic for determining their origin. In particular, it is important to determine if the islands are depositional features or formed by erosion. . Of the 36 islands identified from the 30 m cell-size bathymetric compilation, we have multi-beam bathymetry data over 14 and boomer seismic across 13 of them. All these images show the islands to be dominantly composed of bedrock. Two examples of islands expressing clear bedrock signatures at their surfaces are shown in Figure 6. In Figure 6a we show Island 3, which was formed within a region of tightly folded Jurassic strata. Folded rock units can be traced from a closure on the eastern bank of the channel, across the channel floor and onto the crest of the island. Similarly in Figure 6b we show the eroded core of a small fold shown by rock ridges within Upper Chalk on the top of island 8. This fold was independently mapped by the BGS. Examples of islands displaying their erosional remnant origin from sub-surface data are shown in Figure 7. In Figure 7a we show Island 6 which is partly masked by modern sandwaves. However, the sub-bottom data clearly shows this is simply a thin veneer which is underlain by southerly dipping Wealden strata, consistent with the independent mapping by the BGS. Therefore whilst there is undeniably later modification, it is superficial compared to the bedrock structure of the island as a whole. In Figure 7b we show a second example of the islands being composed of bedrock – in this case Upper Chalk rocks. Throughout the sub-bottom seismic this rock unit is characteristically void of reflectors both on the channel flanks, channel floor and within the islands themselves. The final example of bedrock reflectivity within the core of an island is island 19, which is composed on Paleogene rocks. Again dipping reflectors, consistent with the independently mapped bedrock dip are seen extending up to the seabed within the island (Figure 7c). Our

391 results thus clearly demonstrate that the streamlined islands are eroded bedrock features on the floor of
392 channels and not depositional forms.

393 *3.5 Island planform shape analysis*

394 Table 2 presents the results of the comparison of the planview shapes to the perfect lemniscate for all the
395 islands and Figure 8 shows a summary plotted according to bedrock type. As an entire population the
396 islands show clear tendency towards lemniscate shape, with three-quarters of them having their widest
397 points upstream of their mid-length (i.e., Xm>0.5; Figure 8a).

398 There are clear differences between the Chalk, Paleogene and other bedrock categories. In general the
399 Paleogene islands are the most similar to each other. Among the islands with the five smallest rms misfit
400 (Islands 19, 21, 23, 20, 3) four of them are made of Paleogene rocks (the other Jurassic rocks, Figure 8d).
401 These softer lithologies therefore appear to have more closely reached the hydrodynamically optimum
402 shape compared to the more competent Chalk bedrock. There are exceptions however, in that the island
403 with the largest misfit (Island 13) is also Paleogene. However, in this case, it also has an anomalous length-
404 to-width ratio and is orientated parallel to the geological strike and so here the rheology of individual
405 bedrock units may be influencing island shape. Explanations for many other islands with poorer misfits can
406 also be found. For example, Island 30 (Figure 5b) does not seem to be a product of the flow conditions
407 alone as it appears to be influenced by the boundary between the Chalk and Lower Cretaceous Upper
408 Greensand and Gault Clay that is also seen in the morphology of the neighbouring bank.

409 Overall the islands found in the Chalk have larger length-to-width ratios (3.2 ± 1.3) than those found in
410 more mixed Paleogene terrigenous sandstone and siltstone beds (3.0 ± 1.5) i.e., the Paleogene islands are
411 typically “fatter” (Figure 8b). We attribute these differences to contrasting skin frictions of the two
412 lithologies in the development of minimum drag during island formation. Averaged over the length-scales
413 appropriate for the observed islands, the chalk bedrock is smoother and so had a lower skin friction per

414 unit area, so the islands carved in it could elongate more compared to those carved in the rougher
415 Paleogene strata.

416 Within the two examples of “island families”, in which small islands appear to have been formed from a
417 larger parent by divide crossings (Islands 28-27-26, Figure 5b and Islands 18-17-8, Figure 5c) the analysis
418 provides interesting results. In both cases, the “parent” islands have L/W ratios are far above the average
419 (4.4 for island 26; 5.3 for island 8) suggesting they had not reached equilibrium which is consistent with the
420 apparent on-going “child” production.

421 4 Discussion

422 *4.1 Catastrophic flood versus fluvial carving*

423 Gupta et al., 2007) presented bathymetric data for part of the central English Channel. Our updated and
424 geographically extended compilation of data, enables us to map the erosional features in the Northern
425 Palaeovalley-Lobourg Channel system all the way from the Dover Strait to its entry into the Hurd Deep. In
426 addition, seismic data provide constraints on sub-seabed structure. This allows us to make the following
427 refined observations in support of a catastrophic flood origin for the Channel River morphology.

428 4.1.1 Northern Palaeovalley and Lobourg Channel geometry

429 One of the more compelling pieces of evidence in support of the megaflood origin of the channel is that it is
430 an anabranching system with bedrock islands found within a lowland (low gradient) setting (Tooth and
431 McCarthy, 2004). Bedrock river systems generally form single-thread channels because incision into
432 resistant material provides bank stabilization (Tal and Paola, 2007). In such systems it is very difficult for
433 rivers to bifurcate because this requires breaching of bedrock drainage divides at the channel margin. Such
434 breaching of divides can only occur if flow in the channels is bankfull, which in our examples would require
435 flow depths of >15 m. Moreover, to erode through divides in bedrock in order to carve a completely new
436 channel requires high bed shear stresses that are unlikely to be attained during normal river flows,

including the high discharges expected during Pleistocene times. Bedrock anabranching systems are rare today, and tend to be found as limited stretches within upland areas (Tooth and McCarthy, 2004). In our study area we show anabranching over a much longer stretch of significantly lower gradients and across more varied bedrock types than any known modern examples. We argue that this points to unusual hydrodynamic conditions.

A second diagnostic feature of the mapped channel is its cross-sectional "box shape" with a more-or-less constant width and depth throughout the ~300 km long mapped section. These properties are directly analogous to other known megaflood channels such as the Souris spillway in Saskatchewan (Kehew, 1982). In periglacial environments, a box-shaped cross-sectional form of channels results from thermal erosion of the banks causing collapse during high discharge events (French, 2007), and this may have been a contributing factor here. In cross-section the main channel is also approximately symmetrical throughout the mapped length. This is unlike that expected for normal fluvial systems which are typically irregular and asymmetric along comparable lengths (Kehew and Teller, 1994). The system also has erosional terraces, as expected for catastrophic flooding systems (Kozlowski et al., 2005). We discount later widening of the Northern Palaeovalley due to tidal scour, as this was shown to have minor erosive potential in neighbouring areas (Mitchell et al., 2013). The study area also shows preservation of subtle features such as the secondary drainages which again points to tidal scour being ineffective at eroding bedrock. Later modification in this way is also inconsistent with the presence and geometries of the mid-channel streamlined islands. We therefore conclude that our observations indicate only minor modification of the channel geometry since formation.

4.1.2 Mid-channel islands

The islands within the main channel have been previously interpreted as sand bars (James et al., 2007). However, it is clear from both the seismic and bathymetry data that the islands are composed of bedrock and therefore represent erosional rather than depositional features. Further, these streamlined forms are

surrounded by channel-floor bedrock scours which are consistent with carving by high-magnitude water flows. Our detailed analysis of island shape also shows a correlation with bedrock type, which further suggests they are primary features associated with channel incision rather than later modifications/additions. This is a critical observation in discriminating the English Channel islands from those in modern rivers on neighbouring continents such as the Loire River (Detriche et al., 2010). It is well-known that many European rivers reacted to Quaternary glaciations by periods of incision, particularly during periods when the vegetation was adjusting to the changing climate (Mol et al., 2000). However these episodes typically down-cut a few metres into earlier-deposited, unconsolidated material, whereas to form the islands in our study area required down-cutting of up to 30 m into bedrock.

We compare the results of our shape analysis of the English Channel islands to those published in the literature in Table 3. In this table it can be seen that islands in modern rivers are consistently more elongated than either the English Channel or known megaflood examples, with L/W ratios exceeding 3.5 in rivers and less than 3.5 in megafloods. An exception to this are the islands found in the Marshall River (Tooth and Nanson, 2000), but these may be anomalous as they are formed by ephemeral flows in an area where island development appears to be heavily influenced by vegetation. The English Channel islands are very similar in size to those of the Channeled Scablands, with lengths ranging between 1 and 20 km; whilst they are generally larger than other megaflood examples. Fitting a power-law to our entire length and width population gives a correlation coefficient of 69%, which is only slightly lower than the two previously published examples. This shows that the streamlining process is scale invariant as expected. Our analysis of island shapes therefore demonstrates that the population as a whole are close to true lemniscates which are directly comparable to those found in other well-studied megaflood terrains.

The distribution of the islands is also consistent with the megaflood model. In ordinary rivers, islands tend to form below the joining of tributaries or below valley constrictions (Osterkamp, 1998). Neither of these configurations are seen in the Northern Palaeovalley. The Solent River (which was a major English river

485 during the Pleistocene, Gibbard and Lewin, 2003) has no apparent effect on island distribution, and a
486 numerous set of islands (Group 4) are found upstream of the main confluence with the Southern
487 Palaeovalley.

488 A separate line of argument for carving by a megaflood is the existence of the islands at all, given our study
489 area lies under water today. Within regular river systems, unconsolidated mid-channel islands are
490 inherently unstable and are subject to erosion by flooding and channel migration (Osterkamp, 1998).
491 Indeed in his review of river islands, Osterkamp, 1998 states that relic islands due to catastrophic flooding
492 are the only category that are stable over long time periods. The fact that this area experienced repeated
493 marine transgression makes the preservation of the islands even more remarkable, especially if they are as
494 old as 350-450 ka. In places, particularly in the Weald and Hampshire Basin sections, the seafloor has
495 significant unconsolidated sediment. Published OSL and 14C ages of this material range between ~180 ka
496 and 5 ka and hence records deposition during the past two glacial cycles (Mellett et al., 2013). Indeed we
497 believe that once formed, the entire bedrock-carved channel system was probably fully infilled with fluvial
498 sediments during low sea-level stands. The current exhumation of the bedrock topography is therefore due
499 to the removal of this unconsolidated infill by tidal processes during high-stands. Strong support for this
500 idea comes from the correlation between the unfilled portions of the Northern Palaeovalley with the
501 highest predicted tidally-induced seabed shear stress (Figure 3). Thus the later fluvial sediment infill may
502 have protected the megaflood morphology from modification from both periglacial processes and during
503 the various marine transgressions that followed.

504 ### 4.1.3 Tributaries

505 Three tributaries are seen joining the Northern Palaeovalley, one of which represents the trace of the late
506 Quaternary Solent River, one of which can be correlated to the present-day Arun River and one of which
507 can be correlated to the present-day Canche River (Figure 3c). The French example however is largely
508 obscured by modern sediment, so we do not make any further inferences from it. We do not see the

confluences of the other modern rivers (Adur, Ouse, Cuckmere and Rother) but this is likely due to the complete infilling of these lowstand valleys with sediment.

Neither the Palaeo-Solent nor Palaeo-Arun are graded to the Northern Palaeovalley. Rather both tributaries are sharply truncated by the margin of the Northern Palaeovalley which results in a hanging valley geometry. In the case of the Solent, the mouth of the tributary is raised 10 m above the main channel floor (Figure 9a,c) and in the case of the Arun it is raised 8 m. At this scale, this geometry is most commonly seen when the base level of the main channel drops suddenly and there is insufficient time for the tributary rivers to adjust to the new condition (Komatsu et al., 2009). Hence the observed geometry is entirely consistent with rapid baselevel drop in the Northern Palaeovalley by flood erosion.

In contrast to the tributaries described above, there is another, particularly well-developed large dendritic tributary system offshore of the Weald area of England (labelled "Blind tributary" in Figure 3c, Figure 9b,d). This system is incised into a prominent 20-km-wide bedrock platform that lies at water depths of ~25-30 m. It consists of a network of elongate valleys, up to ~600 m wide that extend ~40 km upstream from their confluence with the Northern Palaeovalley. Importantly the valley network heads on the platform and shows no connection to onshore drainage indicating that it was initiated on the platform itself (Figure 9b). The valley is partly filled by modern mobile sediment in the form of sandwaves, but overall the along-valley profile grades gently into the main channel without a hanging valley as seen in the other examples (Figure 9c). In modern-day jokulhlaups early stage sheet floods evolve into periods of channel deepening during waning flow (Gibling, 2006). Based on this observation, we propose that the bedrock platform represents an initial flood erosion surface that formed a broad spillway in the Strait, prior to subsequent incision of the Lobourg Channel.

4.2 Contribution to our understanding of megaflooding

Significant advances have been made in our understanding of terrestrial megaflooding over the past 40 years. However, there remain several challenges to understanding the process. Firstly, there are a large

number of variables, which include the properties of the inundated landscape (pre-outburst topography and composition) and those of the water flow itself (flood duration, magnitude, depth, density and hydrodynamics). Secondly whilst the identification of the megaflood phenomena is growing, there remain relatively few well-documented terrestrial examples – arguably too few given the number of process variables – from which to draw firm conclusions. Thirdly, the relatively small size and different thermal regimes of modern ice-age glaciers compared to those during ice-ages pose problems of extrapolation to the past conditions of major continental glaciations (Baker, 2009b). However, comparing the overall form of the English Channel example with published maps and photographs from other known megaflood terrains (e.g., Baker and Nummedal, 1978; Elfstrom and Rossbacher, 1985; Kehew and Lord, 1986; Rudoy, 2002; Baker, 2009b; Burr et al., 2009; Meinsen et al., 2011) shows some interesting similarities and differences. We summarise these comparisons below, starting with the terrains that are least similar to the English Channel situation and ending with the terrain that is most similar.

The most diagnostic feature of megaflooding in the English Channel is its streamlined islands. However, not all megaflood terrains contain such features. In the Altai Mountains of Siberia, for example, floods produced extensive deposits (Rudoy and Baker, 1993), including streamlined bars, but large erosional streamlined forms are largely absent (Burr et al., 2009). This has been interpreted as due to the channelization of floodwaters down previously incised river valleys (Herget, 2005). If this inference is correct, then it would be consistent with the English Channel situation, in that prior to the opening of the Dover Strait the English Channel landscape would likely have comprised a drainage network comprised of rivers such as the Palaeo-Solent, Seine and Somme, flowing across a low relief, relatively weakly-incised landscape (Toucanne et al., 2009). The unconfined nature of the pre-existing landscape in the Channel would therefore not have caused focussing of flood flows through a pre-existing conduit, hence favouring streamlined island formation. Our recognition of the “Blind Tributary” offshore the Weald is consistent with this interpretation.

Our English Channel observations of streamlined islands also make interesting comparisons to those described from Germany (Meinsen et al., 2011). This latter island population is found within 10 km of the spill-point, and spread over a 50 km wide zone and surrounded by a network of channels. This distribution is totally unlike that found in our study area where the islands are all contained within a 9-13 km wide channel. Within the German example chevron shaped islands are also common – something we do not see in the English Channel. In the flume experiments of Komar, 1983, he showed, with other factors being equal; increasing flow magnitude is expected to see a change from chevron to tear-drop shapes. The strong difference in island distribution and morphology therefore implies very different flood configurations at these two locations.

Along the palaeo-margin of the Laurentide ice sheet in central and eastern North America, the floodwater pathways show largely erosional streamlined islands, with only limited depositional gravel bars (Lord and Kehew, 1987; Kehew et al., 2009). Whilst the similarity with the English Channel is stronger than the previously described examples; there are clear differences in the number and distribution of the erosional remnants. In the English Channel case, a key characteristic is that all the islands are contained entirely within a main channel and whilst they form in spatial groups, they generally retain some spatial separation from each other. In the central and eastern North American examples, they seem “more crowded”, with “as much island as channel” along many stretches. Isolated erosional remnants do occur within box-shaped channels like in the English Channel, but they are relatively minor (Kehew et al., 2009). Possibly part of the reason is the different bedrock lithologies. In the English Channel we have Mesozoic and Tertiary sedimentary rocks which have been well lithified due to burial prior to uplift as part of the Alpine basin inversion process. In contrast, in the American case the flood-inundated landscape was made of unconsolidated glacial drift and weakly lithified Mesozoic and Tertiary sediments. However, the “maturity” of the flood-carved landscape may also be a factor. In the study by Kehew and Lord, 1986 which included the Minnesota, Minot, Souris-Hind and Thunder spillways, only around 20% of the islands have approached lemniscate geometry. In the English Channel case, we would put this number at around 50%, suggesting

582 flood-parameters (duration, magnitude, suspended material etc) that resulted in more of the islands
583 reaching the optimum shape.

584 The English Channel streamlined island and channel system has the greatest affinity to the Channeled
585 Scablands of western North America. Here streamlined erosional remnants are carved into pre-flood loess
586 underlain by basalt (Baker, 1978; Baker, 2009a). In making this comparison, it is important to remember
587 that in the English Channel we only have direct evidence of "one arm" or tract of the system (the Northern
588 Palaeovalley). If we extrapolate our findings from the unfilled portions to those completely filled by modern
589 sediments (Figure 2) the English Channel has a very similar overall form to the Channeled Scablands which
590 shows a lacework pattern of tracts. In common with the Scablands we find a suite of features consistent
591 with the megaflooding model at the proposed breach point in the Dover strait. These features will be
592 discussed in future companion papers. The streamlined islands themselves compare well on both an
593 individual basis (Figure 10a) and in terms of their spatial relationships to each other and surrounding
594 crescent-shaped scour marks (Figure 10b). The islands compare in physical scale, shape and their
595 characteristic sharp margins. In the English Channel case the islands are typically 2-20 km long, 0.5-10 km
596 wide and 10-20 m high; compared to 1-20 km, 0.5 km and 50 m respectively for the Scablands. As a
597 population, their length-to-width ratios are directly comparable, and their closeness in form to the
598 lemniscate loop is a shared attribute. A difference, however, is the presence of coarse-gravel depositional
599 pendant bars in the Scablands case. If these were produced in the English Channel case they have since
600 been eroded. In both areas the islands also occur in local clusters, organised in a plait-like pattern and with
601 divide crossing separating individual islands.

602 # 5 Conclusions

603 The following conclusions can be drawn from our analysis of the geometry and spatial distribution of the
604 streamlined islands identified from new seafloor and sub-bottom imagery in the Northern Palaeovalley and
605 Lobourg Channel:

1. The streamlined islands are seen throughout the ~300 km mapped section and are composed of bedrock and so are erosional remnants rather than depositional features.

2. The islands display classic lemniscate or tear-drop outlines, with elongated tips pointing downstream, typical of streamlined islands formed during high-magnitude water flow. The length-to-width ratio for the entire island population is 3.4 ± 1.3 and the degree-of-elongation or k-value is 3.7 ± 1.4. These values are comparable to streamlined islands in other proven Pleistocene catastrophic flood terrains and are distinctly different to values found in modern-day rivers

3. Both island geometry and spatial distribution is strongly controlled by seabed geology. In particular, islands carved into more homogeneous and competent Upper Cretaceous Chalk rocks display greater elongation, a bigger population, but less perfect lemniscate shapes than those carved into heterogeneous and softer Paleogene rocks.

4. The islands are similar in scale, geometry and distribution to those identified in other megaflood terrains. This similarity suggests that the islands observed in the study area and carved into bedrock were formed by similar high-energy flows of water to those described in catastrophic flood terrains in the literature.

5. Our analysis of the mid-channel islands, together with the channel and distributary morphologies, strongly supports the megaflood origin for the Channel River system.

6 Acknowledgements

We thank the *Maritime and Coastguard Agency* (MCA) and Graham Potter of the UK Hydrographic Office (UKHO) for providing unprocessed swath and single beam bathymetry data in UK waters. We also thank *Le Service Hydrographique et Océanographique de la Marine* (SHOM) for providing single-beam bathymetric data in French waters (Contract No. 205/2011). We acknowledge the CNRS-INSU for providing shipping time for the DANGEARD 1 cruise aboard Sepia II R/V. Sub-bottom data were also collected under UK's Marine Aggregate Levy Sustainability Fund and we thank Jason Sadler GeoData Institute and Peter Edmonds of the Crown Estate for help with data access. The seismic data were processed using ProMax software available via a software grant to Imperial College London from Landmark Graphics. We also used Kingdom Suite interpretation software made available via a software grant to Imperial College London from IHS Energy. We use digital bedrock geology data which is reproduced with the permission of the British Geological Survey ©NERC. We thank Philip Gibbard and two anonymous referees for their insightful comments on an earlier version of the manuscript.

7 Contributions

JC and SG initiated the project. DGM, AT and MdB provided both bathymetric and seismic data. FO and JC conducted the analysis. All authors discussed the analysis and broader implications. JC wrote the paper with contributions from all other authors.

8 Figure Captions

Figure 1 Topographic map of the English Channel region showing location of the study area (black box) plotted with a WGS-1984 projection. Onshore elevation is from SRTM (Farr et al., 2007) and offshore bathymetry is from GEBCO, 2008. The Quaternary glacial limits are from Ehlers et al., 2011. Inset shows a cartoon of the proglacial lake extent leading to initial breaching of the Strait of Dover, as envisaged for the early stages of maximum Elsterian-Anglian.

649 **Figure 2** Map of the eastern English Channel showing locations of digital datasets used in this study. An
650 interpretation of the data from the Dover Strait region is given elsewhere but is shown here for reference. See
651 text for further details. The background image is the interpretation of the Channel River system of Smith, 1985
652 showing buried (black) and unburied (hachures) elements which was based on the map of Auffret et al., 1980. LC
653 is Lobourg Channel. Modern day, and offshore extensions, of selected rivers are labelled (R. being an
654 abbreviation for River).

655 **Figure 3** (a) New 30m cell-size bathymetric map of the eastern English Channel. The white box outlines the area
656 previously presented in Gupta et al., 2007 and the labelled profiles the cross-sections shown in part b. (b)
657 Bathymetric cross sections. The black arrows indicate our interpretation of the channel margins and red arrows
658 those of an outer channel (where present). The blue lines indicate our interpretation of the margins of the mid-
659 channel islands. (c) Interpretation of and English Channel River features (black annotation) and bedrock geology
660 (red annotation). The mid-channel islands that are the focus of this paper are coloured solid black, with larger
661 islands numbers in white. IG is an abbreviation for "Island Group", as described in the text. The UK onshore
662 geology is from DiGMapGB 1:625,000 (Smith, 2011) and the French onshore geology is based on Bureau de
663 Recherches Géologiques et Minières maps (1:250,000 BRGM, 1979 and 1:1,000,000 BRGM, 2003). The unit
664 labelled Reading Beds are known as the Thanet Beds in the London Basin and Sables et grès d'Ostricourt and
665 Argile de Louvil in northern France. The French Argile des Flandres unit is taken as equivalent to London Clay.
666 Note that the Purbeck Beds actually straddle the Jurassic/Cretaceous boundary but for convenience here and
667 through this paper they are assigned to the "Jurassic" division. The offshore bedrock geology was mapped
668 following the methods described in Collier et al., 2006 and ground truthed by BGS digital 1:250,000 solid geology
669 map sheets Thames Estuary (BGS, 1989), Dungeness-Boulogne (Melville and Freshney, 1982) and Wight (BGS,
670 1995). The UK geological data are reproduced with the permission of the British Geological Survey ©NERC (All
671 rights Reserved). See Table 1 for a summary of lithology within the various mapped units. (d) Interpretation of
672 and English Channel River features overlain the modern-day maximum seabed shear stress resulting from tidal

673 currents calculated with the "Imperial College Ocean Model" (Mitchell et al., 2010). Note the correlation
674 between the model predictions are the best-swept/ most-sedimented stretches of the system. This implies that
675 tidal strength is a key factor in exhuming the mid-channel islands from later channel sediment infill. The four
676 island groups are arbitrary coloured.

677 **Figure 4** Island planform shape analysis. (a) Interpretation of island 20-24 outlines from bathymetric slope
678 calculated from the 30 m cell grid, and (b) Bathymetric contours. (c) Outline of Island 21 with shape definitions.
679 (e) Comparison between calculated streamlined lemniscate (red line, calculated according to Komar, 1984) and
680 island outline (blue line).

681 **Figure 5** Detailed bathymetric views and cross-sections of the Northern Palaeovalley channel and mid-channel
682 islands. (a) Group 4 islands 32-36. (b) Group 3 islands 22-31. (c) Group 2 islands 8 and 15-18. Islands referred to
683 in the text are numbered. According to Komar, 1983, the elongation axis of the islands can be used as a palaeo-
684 flow indicator.

685 **Figure 6** Examples of mid-channel islands showing bedrock structures at the seabed. (a) Islands 2-4 which lie in a
686 part of the channel that cuts through structurally complex Jurassic Kimmeridge Clay/Portland
687 limestones/Purbeck limestones (brown) and Lower Cretaceous Wealden Beds (green) bedrock. Local folding of
688 Jurassic strata west of the channel is seen extending across the floor of the channel on onto the top of Island 3
689 (marked with black arrows). Island 4 also shows bedrock ridges across its top surface which are also seen on the
690 floor of the neighbouring channel floor and hosts a textural change consistent with the BGS map. (b) Island 8
691 shows the clear core of a fold structure within the Upper Chalk bedrock (pale green with brick ornament) which
692 was also been independently mapped by the BGS.

693 **Figure 7** Examples of mid-channel islands showing bedrock structures in the subsurface. (a) Island 6. The bulk of
694 this island lies within the Hastings Beds of the Wealden Group rocks, with the downstream tail crossing into the
695 Lower Greensand Group. (b) Island 15, which is entirely within Upper Chalk. (c) Island 19 which is half within the

696 Paleogene upper London Clay (yellow) and half within the lower Bracklesham Beds (orange, stippled). The base
697 of the latter has a coarse pebble bed of flint pebbles, and it is this unit which may be seen by the rough texture
698 in the bathymetry.

699 **Figure 8** Summary of island lemniscate shape analysis colour-coded according to bedrock type. The histograms
700 show the distribution of (a) locations of the maximum width or "shape factors" (Xm) (b) the length-to-width
701 ratios (L/W) (c) the "elongation factors" ($k = (\pi * L^2)/(4A)$, where A=planform area) and (d) the misfits. See Table 2
702 for raw data.

703 **Figure 9** Comparison of the morphologies of two tributaries – the Palaeo-Solent and "Weald". The Weald system
704 is shown at two scales – the 30 m merged DEM and a 7m MBES DEM. The white lines show the along-valley
705 profiles shown in part (c). NPV=Northern Palaeovalley. The Palaeo-Solent profile contains a distinct step at the
706 boundary between the Upper and Lower Cretaceous bedrock. We interpret this as a fossil-cliff line, with the
707 hanging valley geometry due to the rate of coastline retreat (horizontally) exceeding that of valley channel
708 incision rate (vertically) in the very-low permeability Chalk.

709 **Figure 10** Comparison of the streamlined islands formed in the English Channel to those of the Channeled
710 Scablands (a) Comparison of the planform shapes of individual islands The two English Channel islands carved
711 into Paleogene rocks (right-hand side) show more perfect lemniscate shape but lower elongation (k) values than
712 those carved into Chalk rocks (left hand side). The streamlined islands found in the Channeled Scablands (Baker,
713 1978) are most similar to those found in the English Channel. (b) Comparison of the spatial groupings of islands.
714 The map of the Cheney-Palouse track of the Channel Scablands example is taken from Baker, 2009a.

715 **Table 1** Overview of bedrock geology exposed at the seabed within the study area. Thicknesses and lithologies
716 are taken from the relevant British Regional Geology reports (Gallois, 1968; Melville and Freshney, 1982). In
717 practice, insufficient seabed sampling means that offshore the stratigraphic sub-groups shown here are often
718 undifferentiated (Hamblin et al., 1992). This is particularly true in the Channel and Central Channel Basins. Note

719 that the Purbeck Beds actually straddle the Jurassic/Cretaceous boundary but for convenience here and through
720 this paper they are assigned to the "Jurassic" division. The units equivalent to the Reading Beds are known as the
721 Thanet Beds in the London Basin and Sables et Gres d'Ostricourt and Argile de Louvil in northern France. The
722 French Argile des Flandres unit is taken as equivalent to London Clay.

723 **Table 2** Results of the English Channel island planform shape analysis. See Figure 8 for summary plots of this
724 data.

725 **Table 3** Comparison of English Channel island planform shape parameters with those of other known megaflood
726 terrains on Earth, modern rivers and Mars. The table compares length (L) and width (W) relationships together
727 with Komar's elongation (k) and shape (Xm) factors. Note that in this compilation of known megaflood terrains
728 we have excluded the British Columbian example published by McClenagan, 2013 due to uncertainties as to
729 whether these islands were formed in a sub- rather than pro-glacial setting as our comparison requires (Stumpf
730 et al., 2014). Values are given as mean (standard deviation) where available. Missing data is indicated as "ng"
731 (not given).

732 9 References

733 Alho, P., A. J. Russell, J. L. Carrivick & J. Kayhko, 2005. Reconstruction of the largest Holocene jokulhlaup within
734 Jokulsa a Fjollum, NE Iceland. *Quaternary Science Reviews* **24**, 2319-2334.
735 Auffret, J. P., D. Alduc, C. Larsonneur & A. J. Smith, 1980. Maps of the paleovalleys and of the thickness of
736 superficial sediments in the eastern English-Channel. *Annales de L'Institut Oceanographique* **56**, 21-35.
737 Baker, V. R., 1978. Large-scale erosional and depositional features of the Channeled Scabland. *In* The Channeled
738 Scabland. *Ed.* V. R. Baker and D. Nummedal. Washington, DC, NASA, pp. 81-115.
739 Baker, V. R., 2009a. The Channeled Scabland: A retrospective. *Annual Review of Earth and Planetary Sciences* **37**,
740 393-411.
741 Baker, V. R., 2009b. Overview of megaflooding: Earth and Mars. *In* Megaflooding on Earth and Mars. *Ed.* D. M.
742 Burr, P. A. Carling and V. R. Baker. Cambridge, Cambridge University Press, pp. 1-9.
743 Baker, V. R. & D. Nummedal, 1978. The Channeled Scabland. Washington, DC, NASA pp. 186.
744 Baynes, E. R. C., M. Attal, S. Niedermann, L. A. Kirstein, A. J. Dugmore & M. Naylor, 2015. Erosion during extreme
745 flood events dominates Holocene canyon evolution in northeast Iceland. *Proceedings of the National*
746 *Academy of Sciences of the United States of America* **112**, 2355-2360.
747 BGS, 1989. Thames Estuary. 1:250 000 Solid Geology. Keyworth, British Geological Survey**.**
748 BGS, 1995. Wight. 1:250 000 Solid Geology. Edinburgh, Scotland, British Geological Survey**.**

749 Bourillet, J. F., J. Y. Reynaud, A. Baltzer & S. Zaragosi, 2003. The 'Fleuve Manche': the submarine sedimentary
750 features from the outer shelf to the deep-sea fans. *Journal of Quaternary Science* **18**, 261-282.
751 Bretz, H. J., 1923. The Channeled Scabland of the Columbia Plateau. *Journal of Geology* **31**, 617-649.
752 BRGM, 1979. 4, Rouen, Carte géologique de la France au 1:250 000. BRGM, Orléans**.**
753 BRGM, 2003. La nouvelle carte géologique de la France au 1:1 000 000. BRGM, Orléans**.**
754 Burr, D. M., P. A. Carling & V. R. Baker, 2009. Megaflooding on Earth and Mars, Cambridge University Press pp.
755 330.
756 Carrivick, J. L., A. J. Russell, F. S. Tweed & D. Twigg, 2004. Palaeohydrology and sedimentary impacts of
757 jokulhlaups from Kverkfjoll, Iceland. *Sedimentary Geology* **172**, 19-40.
758 Cenderelli, D. A. & E. E. Wohl, 2001. Peak discharge estimates of glacial-lake outburst floods and "normal"
759 climatic floods in the Mount Everest region, Nepal. *Geomorphology* **40**, 57-90.
760 Clarke, G. K. C., D. W. Leverington, J. T. Teller & A. S. Dyke, 2004. Paleohydraulics of the last outburst flood from
761 glacial Lake Agassiz and the 8200 BP cold event. *Quaternary Science Reviews* **23**, 389-407.
762 Clarke, G. K. C. & W. H. Mathews, 1981. Estimates of the magnitude of glacier outburst floods from Lake Donjek,
763 Yukon-Territory, Canada. *Canadian Journal of Earth Sciences* **18**, 1452-1463.
764 Cohen, K. M., P. L. Gibbard & H. J. T. Weerts, 2014. North Sea palaeogeographical reconstructions for the last 1
765 Ma. *Netherlands Journal of Geosciences-Geologie En Mijnbouw* **93**, 7-29.
766 Collier, J. S., S. Gupta, G. Potter & A. Palmer-Felgate, 2006. Using bathymetry to identify basin inversion
767 structures on the English Channel shelf. *Geology* **34**, 1001-1004.
768 Detriche, S., S. Rodrigues, J. J. Macaire, P. Bonte, J. G. Breheret, J. P. Bakyono & P. Juge, 2010. Caesium-137 in
769 sandy sediments of the River Loire (France): Assessment of an alluvial island evolving over the last 50
770 years. *Geomorphology* **115**, 11-22.
771 Dingwall, R. G., 1975. Sub-bottom infilled channels in an area of the eastern English Channel. *Philosophical*
772 *Transactions of the Royal Society A: Mathematical, Physical and Engineering Sciences* **279**, 233-241.
773 Ehlers, J., P. L. Gibbard & P. D. Hughes, 2011. Quaternary Glaciations - Extent and Chronology, Elsevier pp. 1126.
774 Elfstrom, A. & L. Rossbacher, 1985. Erosional remnants in the Baldakatj Area, Lapland, northern Sweden.
775 *Geografiska Annaler Series A - Physical Geography* **67**, 167-176.
776 Farr, T. G., P. A. Rosen, E. Caro, et al., 2007. The shuttle radar topography mission. *Reviews of Geophysics* **45**, DOI
777 10.1029/2005rg000183.
778 French, H. M., 2007. The Periglacial Environment. Hoboken, NJ Wiley pp. 478.
779 Gallois, R. W., 1968. British Regional Geology: The Wealden District. London, Institute of Geological Sciences pp.
780 101.
781 García-Moreno, D., K. Verbeeck, T. Camelbeeck, M. D. Batist, F. Oggioni, O. Z. Hurtado, W. Versteeg, H. Jomard,
782 J. S. Collier, S. Gupta, A. Trentesaux & K. Vanneste, 2015. Fault activity in the epicentral area of the 1580
783 Dover-Strait/Pas-de-Calais earthquake (North-western Europe). *Geophysical Journal International* **201**,
784 528-542.
785 GEBCO, 2008. General Bathymetric Chart of the Oceans - GEBCO_08 Grid, version 20081212. www.gebco.net.
786 Gibbard, P. L., 1988. The history of the great northwest European rivers during the past three million years.
787 *Philosophical Transactions of the Royal Society B: Biological Sciences* **318**, 559-602.
788 Gibbard, P. L., 1995. The formation of the Strait of Dover. *In* Island Britain: a Quaternary perspective. *Ed.*,
789 Geological Society, London, Special Publications. 96 pp. 15-26.
790 Gibbard, P. L. & K. M. Cohen, 2015. Quaternary evolution of the North Sea and the English Channel. *Proceedings*
791 *of the Open University Geological Society* **1**, 65-76.
792 Gibbard, P. L. & J. Lewin, 2003. The history of the major rivers of southern Britain during the Tertiary. *Journal of*
793 *the Geological Society* **160**, 829-845.
794 Gibling, M. R., 2006. Width and thickness of fluvial channel bodies and valley fills in the geological record: A
795 literature compilation and classification. *Journal of Sedimentary Research* **76**, 731-770.
796 Gupta, S., J. S. Collier, A. Palmer-Felgate & G. Potter, 2007. Catastrophic flooding origin of shelf valley systems in

797 the English Channel. *Nature* **448**, 342-345.
798 Gupta, S., J. S. Collier, A. Palmer Felgate, J. Dickinson & K. E. A. Bushe, 2004. The submerged Palaeo-Arun River:
799 Reconstruction of prehistoric landscapes and evaluation of archaeological resource potential. ALSF Final
800 Report to English Heritage**.**
801 Gurnell, A. M. & G. E. Petts, 2002. Island-dominated landscapes of large floodplain rivers, a European
802 perspective. *Freshwater Biology* **47**, 581-600.
803 Hamblin, R., A. Crosby, P. Balson, S. Jones, R. Chadwick, I. Penn & M. Arthur, 1992. United Kingdom Offshore
804 Regional Report: The Geology of the English Channel, British Geological Survey pp. 106.
805 Hamilton, D. & A. J. Smith 1972. The origin and sedimentary history of the Hurd Deep, English Channel,
806 with additional notes on other deeps in the western English Channel. *Mémoires du Bureau de*
807 *Recherches Géologiques et Minières* **79**, 59-68.
808 Herget, J., 2005. Reconstruction of Pleistocene ice-dammed lake outburst floods in the Altai Mountains, Siberia.
809 *Geological Society of America Special Papers* **386**, 1-2.
810 Hijma, M. P., K. M. Cohen, W. Roebroeks, W. E. Westerhoff & F. S. Busschers, 2012. Pleistocene Rhine-Thames
811 landscapes: geological background for hominin occupation of the southern North Sea region. *Journal of*
812 *Quaternary Science* **27**, 17-39.
813 James, J. W. C., R. A. Coggan, S. Blyth & V. J. Morando, 2007. The Eastern English Channel Marine Habitat Map.
814 ALSF Final Report to CEFAS**.**
815 James, J. W. C., B. Pearce, R. A. Coggan, S. H. L. Arnott, R. Clark, J. F. Plim, J. Pinnion, C. Barrio Frójan, J. P.
816 Gardiner, A. Morando, P. A. Baggaley, G. Scott & B. N, 2010. The South Coast Regional Environmental
817 Characterisation. ALSF Final Report to CEFAS**.**
818 James, J. W. C., B. Pearce, R. A. Coggan, M. Leivers, R. W. E. Clark, J. F. Plim, J. M. Hill, S. H. L. Arnott, L. Bateson,
819 A. De-Burgh Thomas & P. A. Baggaley, 2011. The MALSF synthesis study in the central and eastern
820 English Channel. ALSF Final Report to CEFAS**.**
821 Kale, V. S., V. R. Baker & S. Mishra, 1996. Multi-channel patterns of bedrock rivers: An example from the central
822 Narmada basin, India. *Catena* **26**, 85-98.
823 Kehew, A. E., 1982. Catastrophic flood hypothesis for the origin of the Souris Spillway, Saskatchewan and North-
824 Dakota. *Geological Society of America Bulletin* **93**, 1051-1058.
825 Kehew, A. E., 1993. Glacial-lake outburst erosion of the Grand Valley, Michigan, and impacts on glacial lakes in
826 the Lake-Michigan Basin. *Quaternary Research* **39**, 36-44.
827 Kehew, A. E. & M. L. Lord, 1986. Origin and large-scale erosional features of Glacial-Lake spillways in the
828 northern Great-Plains. *Geological Society of America Bulletin* **97**, 162-177.
829 Kehew, A. E., M. L. Lord, A. L. Kozlowski & T. G. Fisher, 2009. Proglacial megaflooding along the margins of the
830 Laurentide Ice Sheet. *In* Megaflooding on Earth and Mars. *Ed.* D. M. Burr, P. A. Carling and V. R. Baker,
831 Cambridge University Press, pp. 104-127.
832 Kehew, A. E. & J. T. Teller, 1994. History of late-glacial runoff along the southwestern margin of the Laurentide
833 ice-sheet. *Quaternary Science Reviews* **13**, 859-877.
834 Komar, P. D., 1983. Shapes of streamlined islands on Earth and Mars - Experiments and analyses of the
835 minimum-drag form. *Geology* **11**, 651-654.
836 Komar, P. D., 1984. The lemniscate loop - comparisons with the shapes of streamlined landforms. *Journal of*
837 *Geology* **92**, 133-145.
838 Komatsu, G., S. G. Arzhannikov, A. R. Gillespie, R. M. Burke, H. Miyamoto & V. R. Baker, 2009. Quaternary
839 paleolake formation and cataclysmic flooding along the upper Yenisei River. *Geomorphology* **104**, 143-
840 164.
841 Kor, P. S. G., J. Shaw & D. R. Sharpe, 1991. Erosion of bedrock by subglacial meltwater, Georgian Bay, Ontario - a
842 regional view. *Canadian Journal of Earth Sciences* **28**, 623-642.
843 Kozlowski, A. L., A. E. Kehew & B. C. Bird, 2005. Outburst flood origin of the Central Kalamazoo River Valley,
844 Michigan, USA. *Quaternary Science Reviews* **24**, 2354-2374.

Lamb, M. P., B. H. Mackey & K. A. Farley, 2014. Amphitheater-headed canyons formed by megaflooding at Malad Gorge, Idaho. *Proceedings of the National Academy of Sciences* **111**, 57-62.

Le Roy, P., C. Gracia-Garay, P. Guennoc, J. F. Bourillet, J. Y. Reynaud, I. Thinon, P. Kervevan, F. Paquet, D. Menier & C. Bulois, 2011. Cenozoic tectonics of the Western Approaches Channel Basins and its control of local drainage systems. *Bulletin De La Societe Geologique De France* **182**, 451-463.

Lericolais, G., J. P. Auffret & J. F. Bourillet, 2003. The Quaternary Channel River: seismic stratigraphy of its palaeo-valleys and deeps. *Journal of Quaternary Science* **18**, 245-260.

Lericolais, G., J. P. Auffret, J. F. Bourillet, S. Berne, P. Guennoc, E. Ledrezen, A. Normand & F. Guillocheau, 1995. The enigmatic English-Channel Hurd Deep - Morphological study and sedimentary infill revealed by high resolution geophysical techniques. *Comptes Rendus De l'Académie Des Sciences Série Ii Fascicule A-Sciences de la Terre et des Planètes* **321**, 39-46.

Lericolais, G., P. Guennoc, J. P. Auffret, J. F. Bourillet & S. Berne, 1996. Detailed survey of the western end of the Hurd Deep (English Channel): new facts for a tectonic origin. *Geological Society, London, Special Publications* **117**, 203-215.

Lord, M. L. & A. E. Kehew, 1987. Sedimentology and paleohydrology of glacial-lake outburst deposits in southeastern Saskatchewan and northwestern North-Dakota. *Geological Society of America Bulletin* **99**, 663-673.

Marshall, S. J. & G. K. C. Clarke, 1999. Modeling North American freshwater runoff through the last glacial cycle. *Quaternary Research* **52**, 300-315.

McClenagan, J. D., 2013. Streamlined erosional residuals and drumlins in central British Columbia, Canada. *Geomorphology* **189**, 41-54.

Meijer, T. & R. C. Preece, 1995. Malacological evidence relating to the insularity of the British Isles during the Quaternary. *In* Island Britain: a Quaternary perspective. *Ed.*, Geological Society, London, Special Publications. 96 pp. 89-110.

Meinsen, J., J. Winsemann, A. Weitkamp, N. Landmeyer, A. Lenz & M. Dolling, 2011. Middle Pleistocene (Saalian) lake outburst floods in the Munsterland Embayment (NW Germany): impacts and magnitudes. *Quaternary Science Reviews* **30**, 2597-2625.

Mellett, C. L., D. M. Hodgson, A. J. Plater, B. Mauz, I. Selby & A. Lang, 2013. Denudation of the continental shelf between Britain and France at the glacial-interglacial timescale. *Geomorphology* **203**, 79-96.

Mellett, C. L., B. Mauz, A. J. Plater, D. M. Hodgson & A. Lang, 2012. Optical dating of drowned landscapes: A case study from the English Channel. *Quaternary Geochronology* **10**, 201-208.

Melville, R. V. & E. C. Freshney, 1982. British Regional Geology: The Hampshire Basin. London, Institute of Geological Sciences pp. 146.

Mitchell, A. J., D. Ulicny, G. J. Hampson, P. A. Allison, G. J. Gorman, M. D. Piggott, M. R. Wells & C. C. Pain, 2010. Modelling tidal current-induced bed shear stress and palaeocirculation in an epicontinental seaway: the Bohemian Cretaceous Basin, Central Europe. *Sedimentology* **57**, 359-388.

Mitchell, N. C., J. M. Huthnance, T. Schmitt & B. Todd, 2013. Threshold of erosion of submarine bedrock landscapes by tidal currents. *Earth Surface Processes and Landforms* **38**, 627-639.

Mol, J., J. Vandenberghe & C. Kasse, 2000. River response to variations of periglacial climate in mid-latitude Europe. *Geomorphology* **33**, 131-148.

Moscardelli, L. & L. Wood, 2011. Deep-water erosional remnants in eastern offshore Trinidad as terrestrial analogs for teardrop-shaped islands on Mars: Implications for outflow channel formation. *Geology* **39**, 699-702.

Murton, J. B., M. D. Bateman, S. R. Dallimore, J. T. Teller & Z. R. Yang, 2010. Identification of Younger Dryas outburst flood path from Lake Agassiz to the Arctic Ocean. *Nature* **464**, 740-743.

O'Connor, J. E., 1993. Hydrology, hydraulics and geomorphology of the Bonneville flood. Geological Society of America Special Paper 274. Boulder, Co. 102**.**

O'Connor, J. E. & V. R. Baker, 1992. Magnitudes and implications of peak discharges from Glacial Lake Missoula.

Geological Society of America Bulletin **104**, 267-279.
Oggioni, F., 2013. Characterization of catastropic flood-related features in the English Channel, PhD thesis, Imperial College London**.**
Osterkamp, W. R., 1998. Processes of fluvial island formation, with examples from Plum Creek, Colorado and Snake River, Idaho. *Wetlands* **18**, 530-545.
Rudoy, A. N., 2002. Glacier-dammed lakes and geological work of glacial superfloods in the Late Pleistocene, Southern Siberia, Altai Mountains. *Quaternary International* **87**, 119-140.
Rudoy, A. N. & V. R. Baker, 1993. Sedimentary effects of cataclysmic Late Pleistocene glacial outburst flooding, Altay Mountains, Siberia. *Sedimentary Geology* **85**, 53-62.
Smith, A., 2011. DigMapGB, British Geological Survey Open Report OR/10/050**.**
Smith, A. J., 1985. A catastrophic origin for the palaeovalley system of the eastern English-Channel. *Marine Geology* **64**, 65-75.
Stumpf, A. J., T. Ferbey, A. Plouffe, J. J. Clague, B. C. Ward, R. C. Paulen & A. B. G. Bush, 2014. Discussion: "Streamlined erosional residuals and drumlins in central British Columbia, Canada" by J. Donald McClenagan, (2013) Geomorphology 189,41-54. *Geomorphology* **209**, 147-150.
Tal, M. & C. Paola, 2007. Dynamic single-thread channels maintained by the interaction of flow and vegetation. *Geology* **35**, 347-350.
Tooth, S. & T. S. McCarthy, 2004. Anabranching in mixed bedrock-alluvial rivers: the example of the Orange River above Augrabies Falls, Northern Cape Province, South Africa. *Geomorphology* **57**, 235-262.
Tooth, S. & G. C. Nanson, 2000. The role of vegetation in the formation of anabranching channels in an ephemeral river, Northern plains, arid central Australia. *Hydrological Processes* **14**, 3099-3117.
Toucanne, S., S. Zaragosi, J. F. Bourillet, P. L. Gibbard, F. Eynaud, J. Giraudeau, J. L. Turon, M. Cremer, E. Cortijo, P. Martinez & L. Rossignol, 2009. A 1.2 Ma record of glaciation and fluvial discharge from the West European Atlantic margin. *Quaternary Science Reviews* **28**, 2974-2981.
Van Vliet-Lanoe, B., J. L. Mansy, J. P. Margerel, J. P. Vidier, J. Lamarche & M. Everaerts, 1998. The Dover Strait, a discretely open Cenozoic strait. *Comptes Rendus De l'Académie Des Sciences Série Ii Fascicule A-Sciences de la Terre et des Planètes* **326**, 729-736.
Vandenberghe, J., 2001. A typology of Pleistocene cold-based rivers. *Quaternary International* **79**, 111-121.
Vandenberghe, J., 2002. The relation between climate and river processes, landforms and deposits during the Quaternary. *Quaternary International* **91**, 17-23.
Westaway, R. & D. R. Bridgland, 2010. Causes, consequences and chronology of large-magnitude palaeoflows in Middle and Late Pleistocene river systems of northwest Europe. *Earth Surface Processes and Landforms* **35**, 1071-1094.
Wiedmer, M., D. R. Montgomery, A. R. Gillespie & H. Greenberg, 2010. Late Quaternary megafloods from Glacial Lake Atna, Southcentral Alaska, U.S.A. *Quaternary Research* **73**, 413-424.
Wyrick, J., 2005. On the formation of fluvial islands. Corvallis, PhD thesis, Oregan State University**.**
Wyrick, J. R. & P. C. Klingeman, 2011. Proposed fluvial island classification scheme and its use for river restoration. *River Research and Applications* **27**, 814-825.

Figure

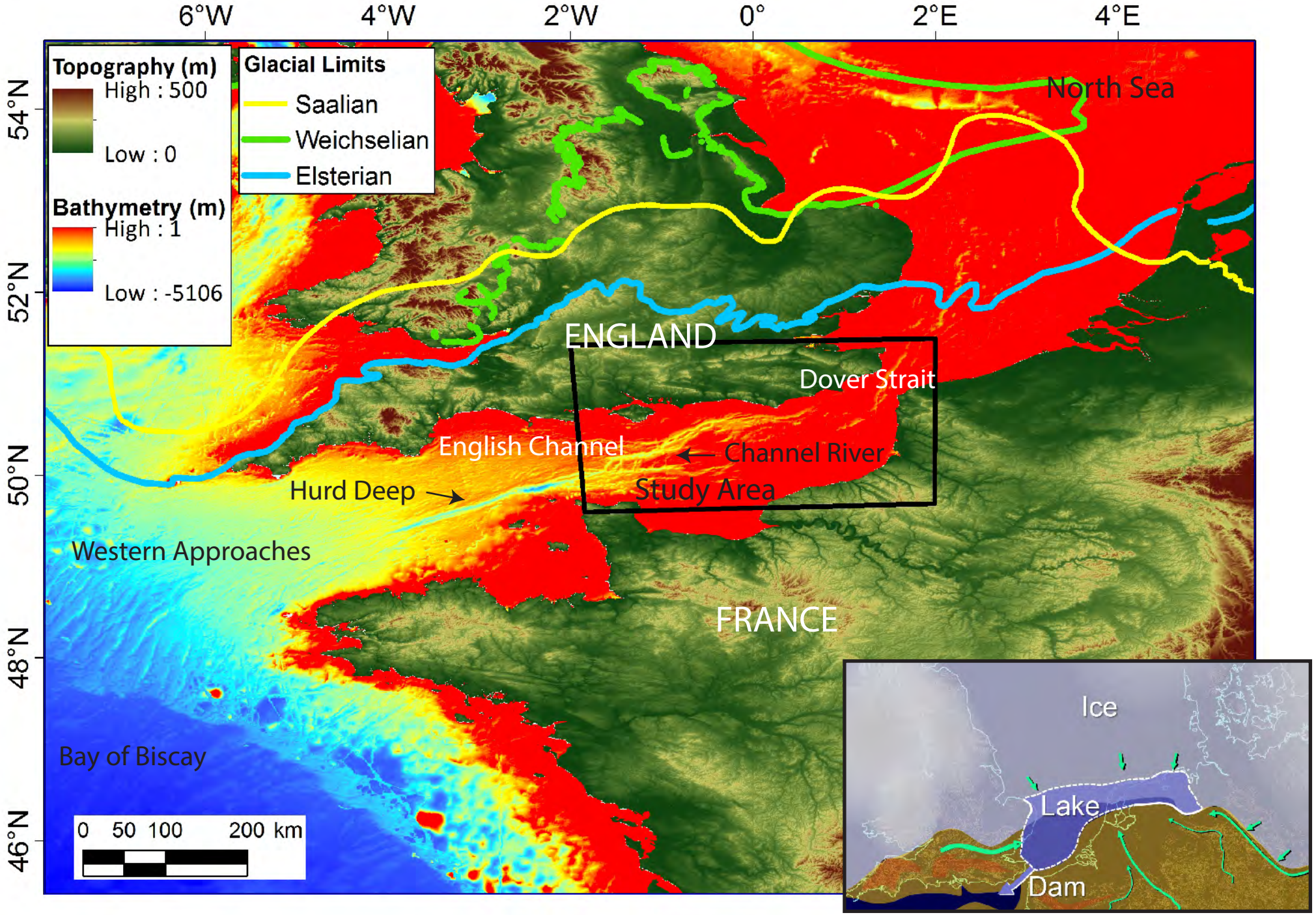


Figure 1

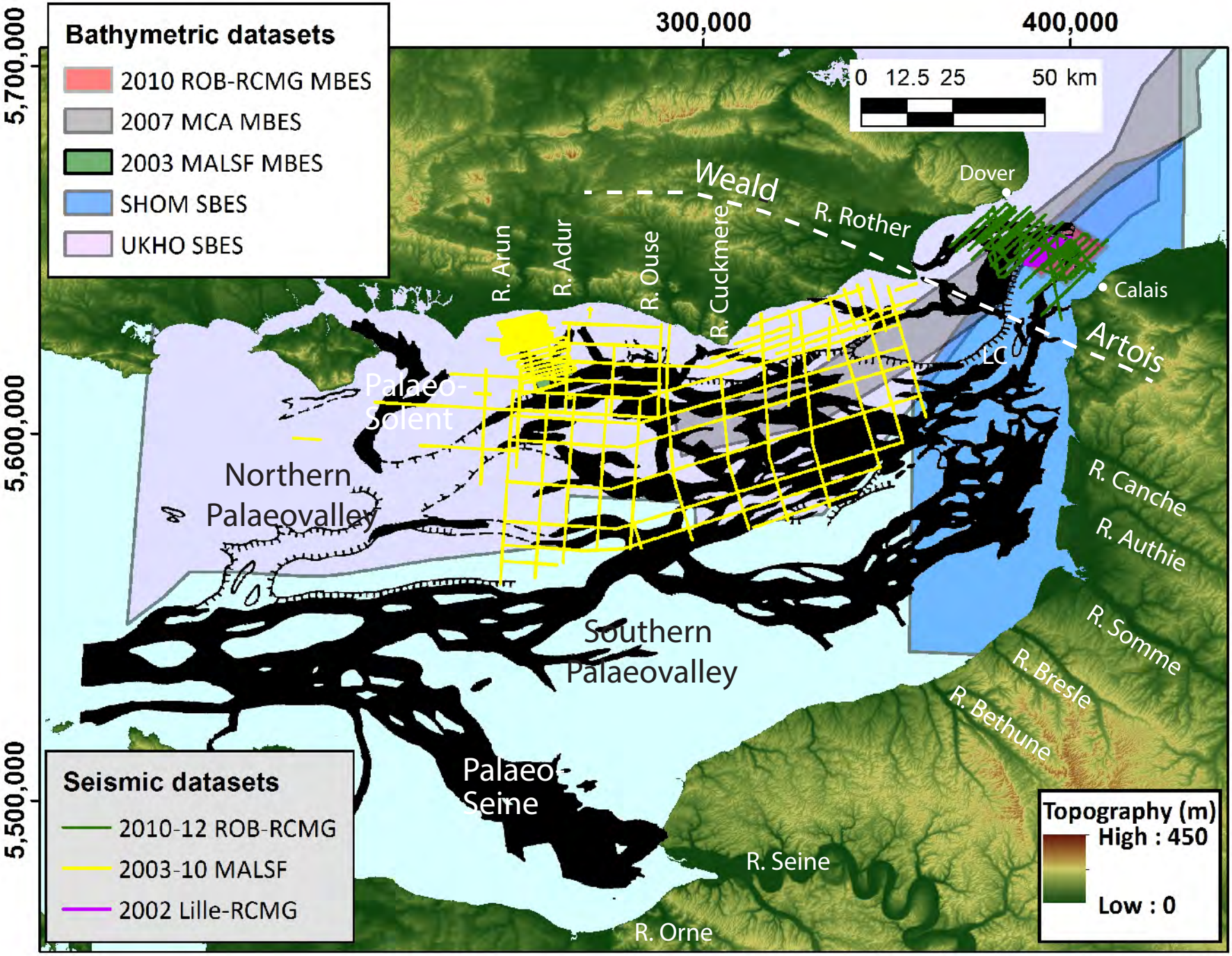

Bathymetric datasets
2010 ROB-RCMG MBES
2007 MCA MBES
2003 MALSF MBES
SHOM SBES
UKHO SBES
300,000
400,000
5,700,000
5,600,000
5,500,000
0 12.5 25 50 km
Weald
R. Rother
Dover
Calais
Artois
LC
R. Arun
R. Adur
R. Ouse
R. Cuckmere
Palaeo-Solent
Northern Palaeovalley
Southern Palaeovalley
Palaeo-Seine
R. Canche
R. Authie
R. Somme
R. Bresle
R. Bethune
R. Seine
R. Orne
Seismic datasets
2010-12 ROB-RCMG
2003-10 MALSF
2002 Lille-RCMG
Topography (m)
High : 450
Low : 0

Figure 2

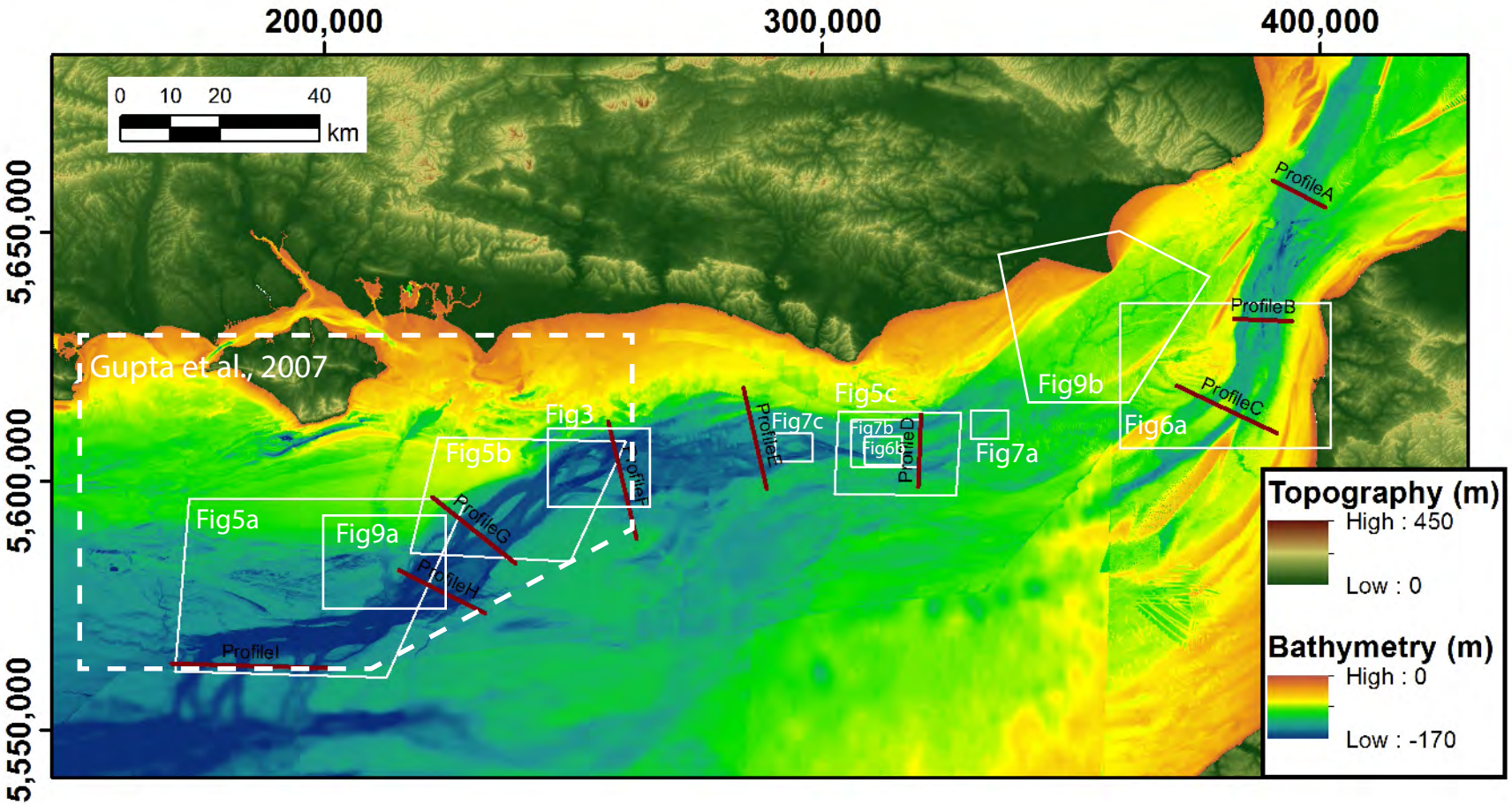

200,000
300,000
400,000
5,650,000
5,600,000
5,550,000
0 10 20 40
km
Gupta et al., 2007
Fig3
Fig5a
Fig5b
Fig5c
Fig6a
Fig6b
Fig7a
Fig7b
Fig7c
Fig9a
Fig9b
ProfileA
ProfileB
ProfileC
ProfileD
ProfileE
ProfileF
ProfileG
ProfileH
ProfileI
Topography (m)
High : 450
Low : 0
Bathymetry (m)
High : 0
Low : -170

Figure 3a

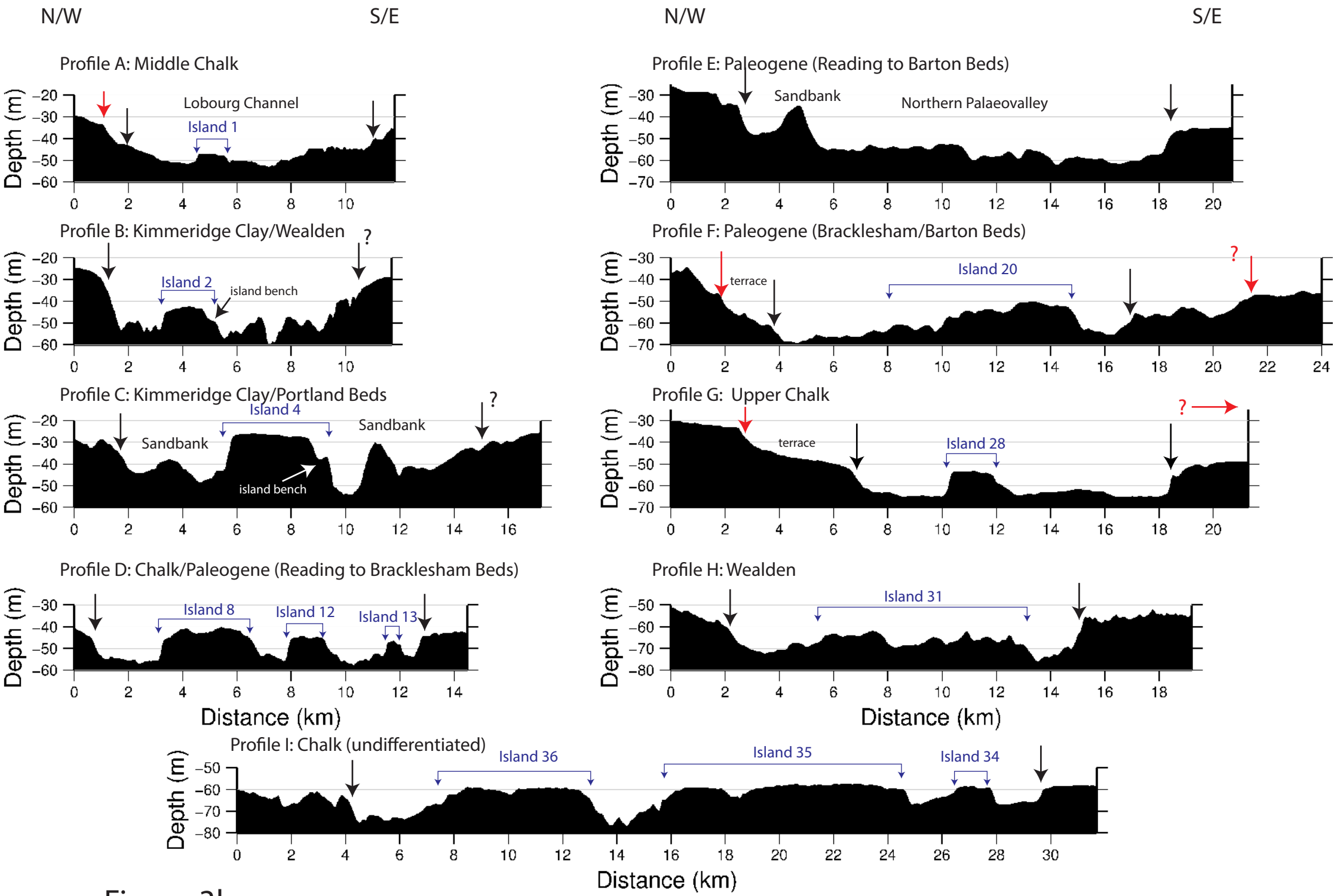

N/W
S/E
Profile A: Middle Chalk
Lobourg Channel
Island 1
Depth (m)
Profile B: Kimmeridge Clay/Wealden
Island 2
island bench
Profile C: Kimmeridge Clay/Portland Beds
Island 4
Sandbank
Sandbank
island bench
Profile D: Chalk/Paleogene (Reading to Bracklesham Beds)
Island 8
Island 12
Island 13
Distance (km)
N/W
S/E
Profile E: Paleogene (Reading to Barton Beds)
Sandbank
Northern Palaeovalley
Profile F: Paleogene (Bracklesham/Barton Beds)
terrace
Island 20
Profile G: Upper Chalk
terrace
Island 28
Profile H: Wealden
Island 31
Distance (km)
Profile I: Chalk (undifferentiated)
Island 36
Island 35
Island 34
Distance (km)

Figure 3b

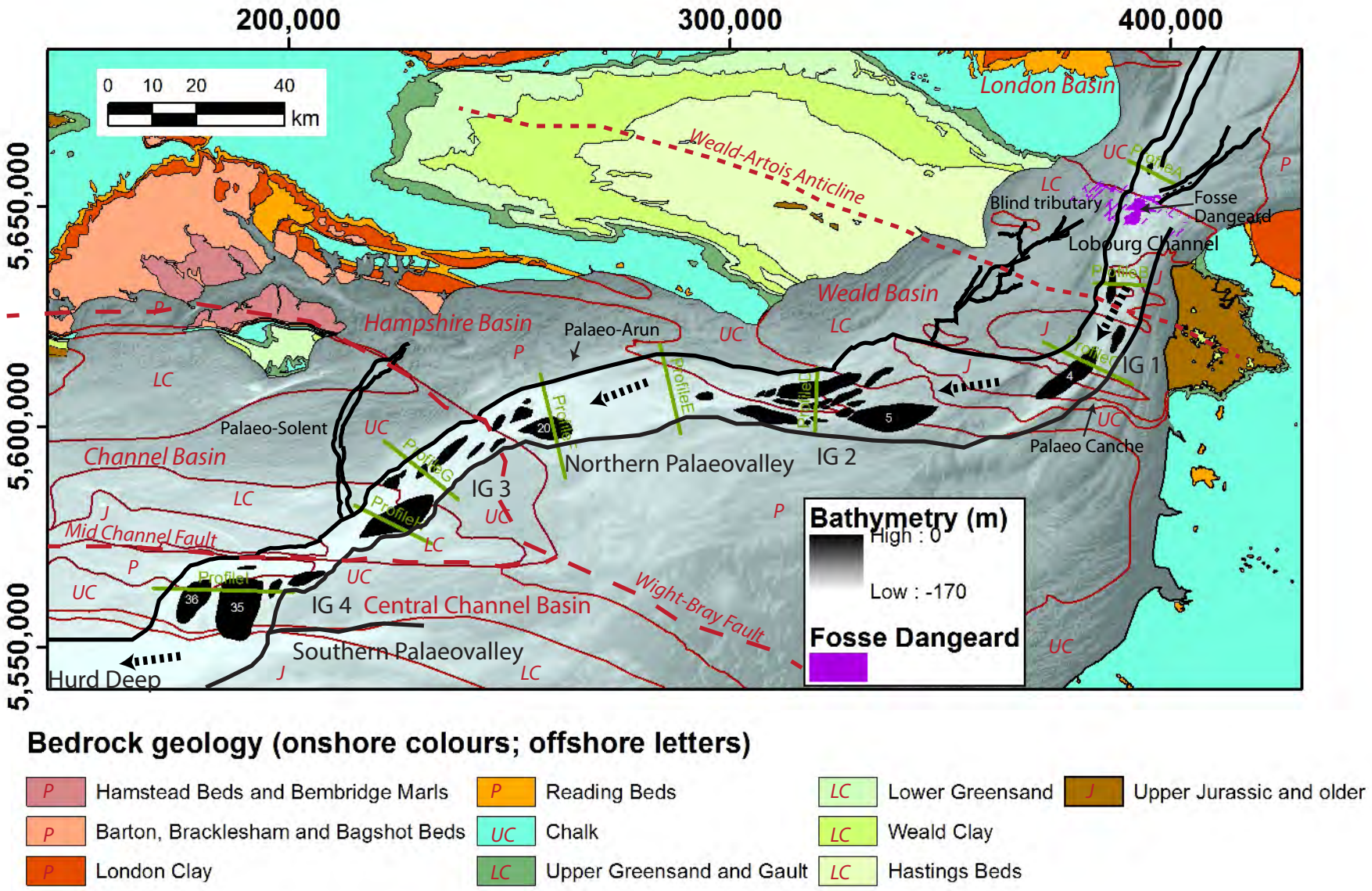

200,000
300,000
400,000
5,650,000
5,600,000
5,550,000
0 10 20 40
km
London Basin
Weald-Artois Anticline
Blind tributary
Fosse Dangeard
Lobourg Channel
Weald Basin
Hampshire Basin
Palaeo-Arun
Palaeo-Solent
Channel Basin
Northern Palaeovalley
IG 1
IG 2
IG 3
IG 4
Central Channel Basin
Southern Palaeovalley
Palaeo Canche
Mid Channel Fault
Wight-Bray Fault
Hurd Deep
ProfileA
ProfileB
ProfileC
ProfileD
ProfileE
ProfileF
Bathymetry (m)
High : 0
Low : -170
Fosse Dangeard
Bedrock geology (onshore colours; offshore letters)
P Hamstead Beds and Bembridge Marls
P Barton, Bracklesham and Bagshot Beds
P London Clay
P Reading Beds
UC Chalk
LC Upper Greensand and Gault
LC Lower Greensand
LC Weald Clay
LC Hastings Beds
J Upper Jurassic and older

Figure 3c

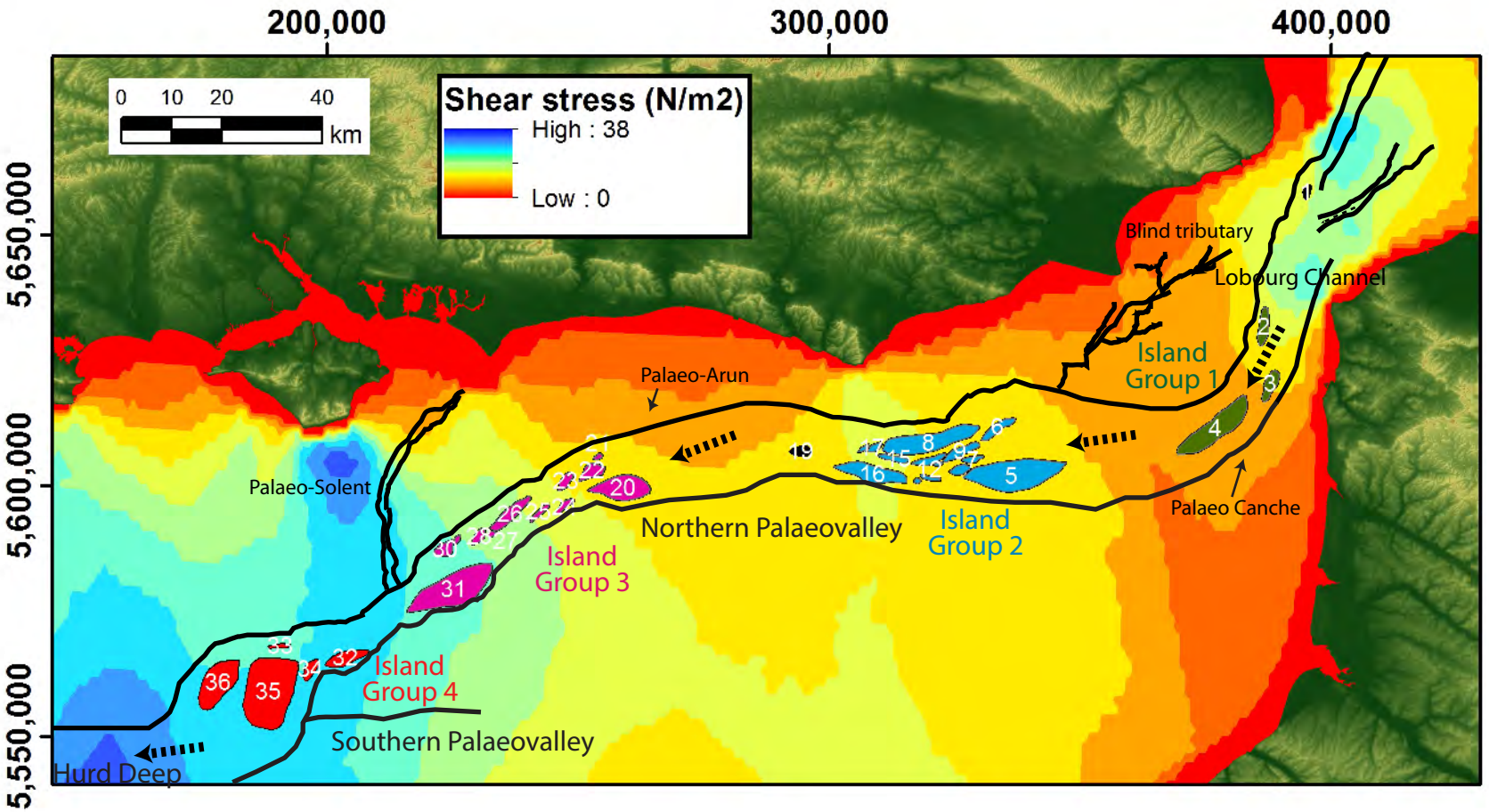
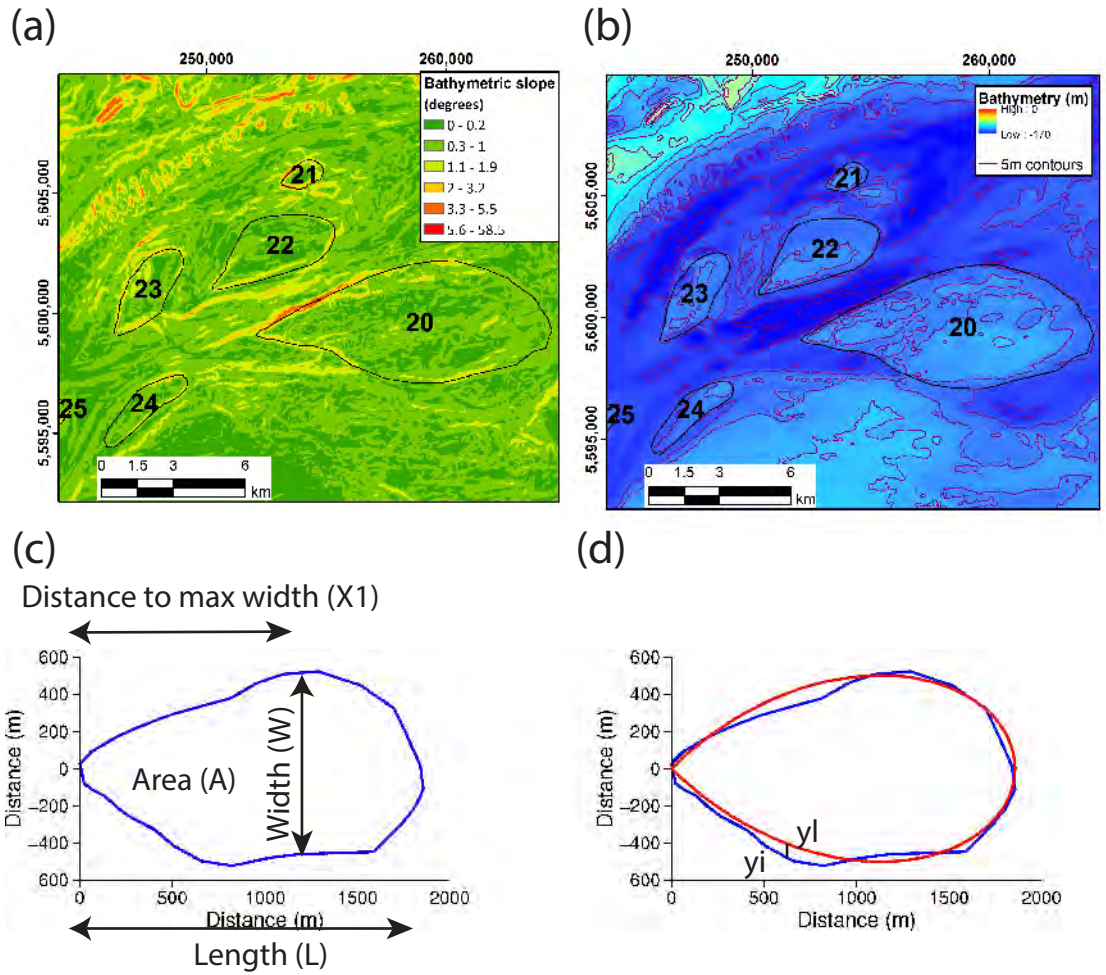

200,000
300,000
400,000
5,650,000
5,600,000
5,550,000
0 10 20 40
km
Shear stress (N/m2)
High : 38
Low : 0
Blind tributary
Lobourg Channel
Island Group 1
Palaeo-Arun
Palaeo-Solent
Palaeo Canche
Northern Palaeovalley
Island Group 2
Island Group 3
Island Group 4
Southern Palaeovalley
Hurd Deep

Figure 3d



Elongation factor, k = (π*L*L)/(4A)

misfit = 100*(average(mod(yi-yl))/average (yl))

Shape factor (Xm) =X1/L

For Island 21: L=1857m, W= 982m, A= 1,344,393 m2; Xm=0.69, k=2.0, misfit=14%

Figure 4

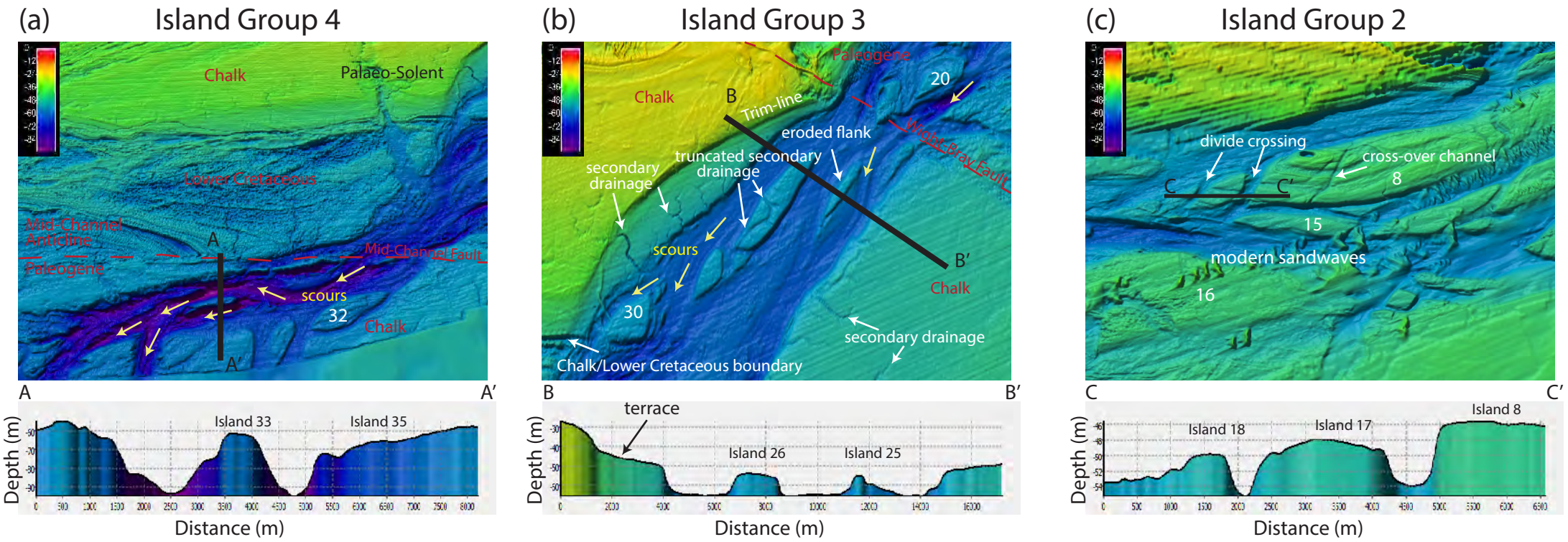

(a)
Island Group 4
Chalk
Palaeo-Solent
Lower Cretaceous
Mid-Channel Anticline
Paleogene
A
Mid-Channel Fault
scours
32
Chalk
A'
A
A'
Depth (m)
Island 33
Island 35
Distance (m)
(b)
Island Group 3
Paleogene
Chalk
B
Trim-line
20
eroded flank
Wight-Fray Fault
secondary drainage
truncated secondary drainage
scours
30
B'
Chalk
secondary drainage
Chalk/Lower Cretaceous boundary
B
B'
terrace
Depth (m)
Island 26
Island 25
Distance (m)
(c)
Island Group 2
divide crossing
cross-over channel
8
C
C'
15
modern sandwaves
16
C
C'
Island 8
Island 18
Island 17
Depth (m)
Distance (m)

Figure 5

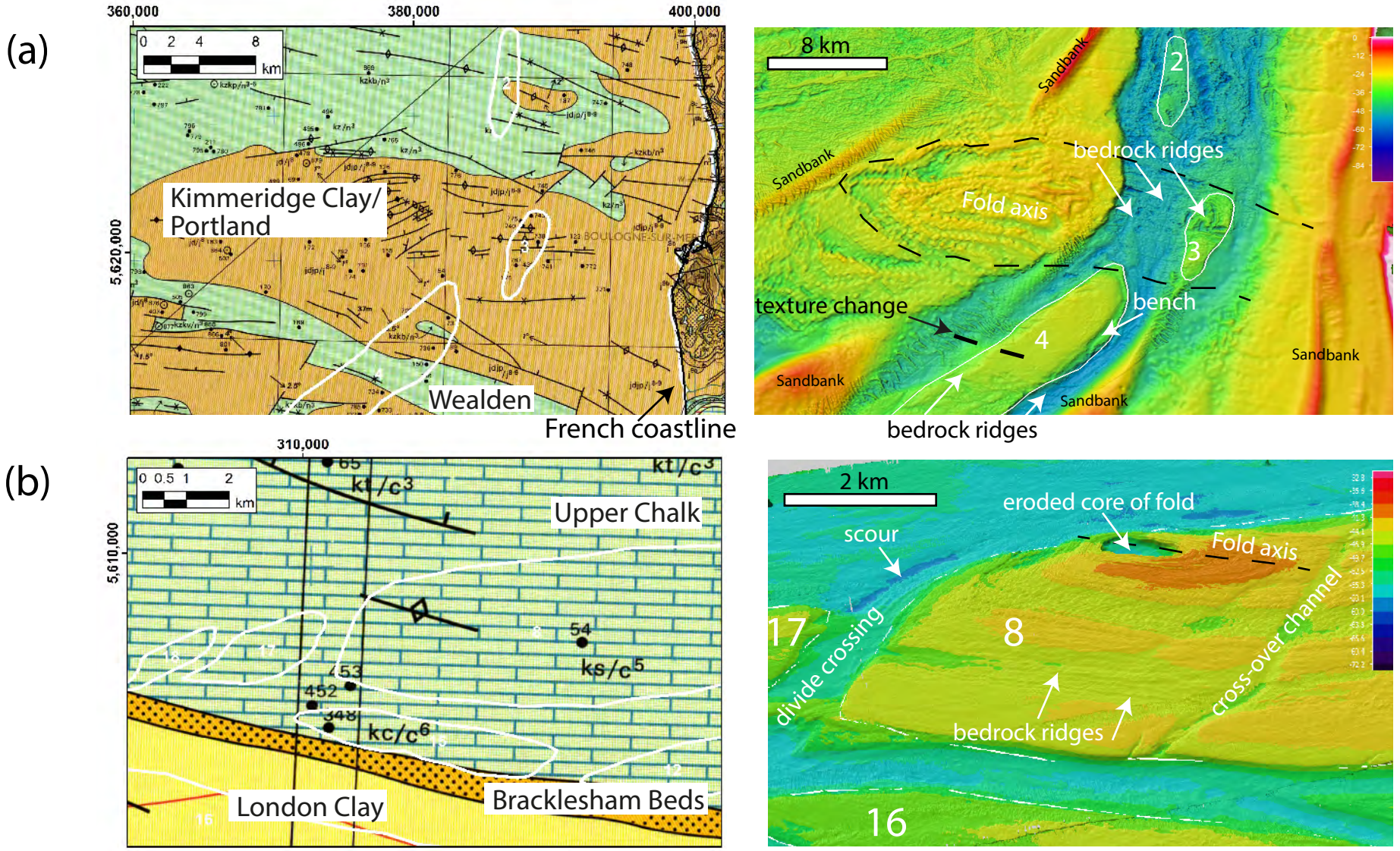

(a)
360,000
380,000
400,000
0 2 4 8
km
5,620,000
Kimmeridge Clay/
Portland
Wealden
French coastline
8 km
Sandbank
2
bedrock ridges
Fold axis
3
texture change
bench
4
Sandbank
Sandbank
Sandbank
bedrock ridges
(b)
310,000
0 0.5 1 2
km
5,610,000
Upper Chalk
kt/c3
ks/c5
kc/c6
London Clay
Bracklesham Beds
2 km
eroded core of fold
scour
Fold axis
17
8
divide crossing
cross-over channel
bedrock ridges
16

Figure 6

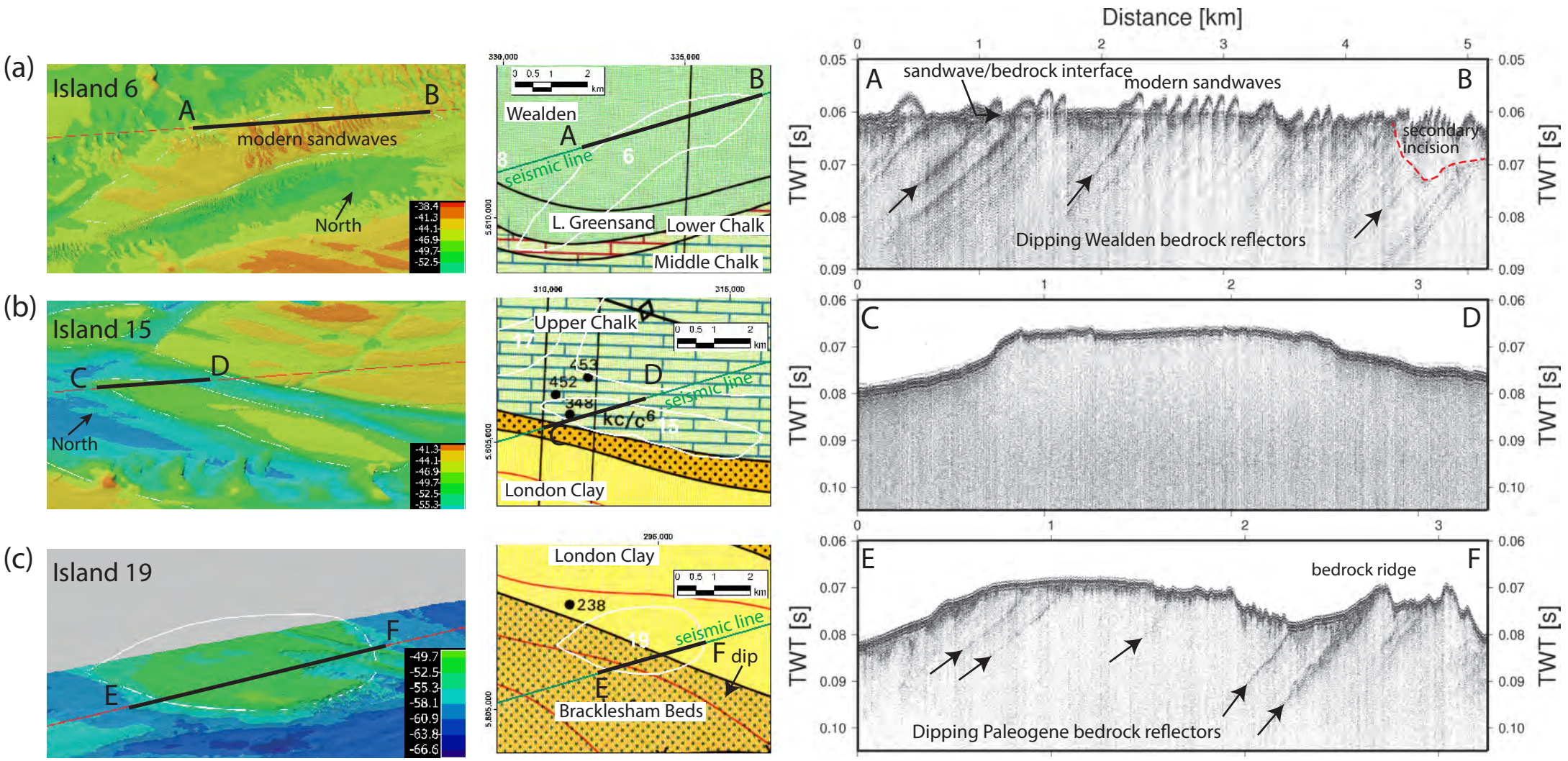

(a)
Island 6
A
B
modern sandwaves
North
-38.4
-41.3
-44.1
-46.9
-49.7
-52.5
Wealden
seismic line
L. Greensand
Lower Chalk
Middle Chalk
(b)
Island 15
C
D
North
-41.3
-44.1
-46.9
-49.7
-52.5
-55.3
Upper Chalk
453
452
348
kc/c6
seismic line
London Clay
(c)
Island 19
F
E
-49.7
-52.5
-55.3
-58.1
-60.9
-63.8
-66.6
London Clay
238
19
seismic line
F dip
Bracklesham Beds
Distance [km]
TWT [s]
sandwave/bedrock interface
modern sandwaves
secondary incision
Dipping Wealden bedrock reflectors
bedrock ridge
Dipping Paleogene bedrock reflectors

Figure 7

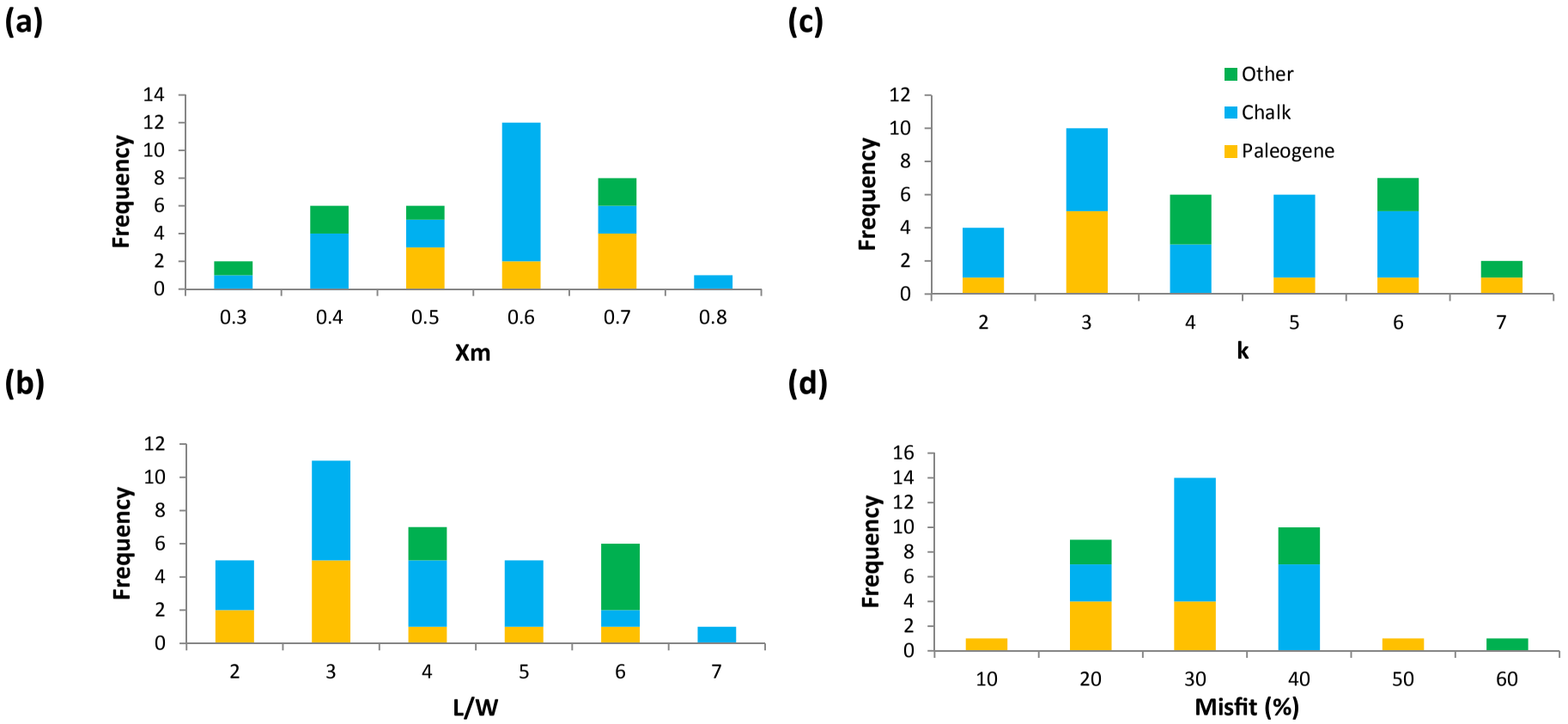

(a)
Frequency
14
12
10
8
6
4
2
0
0.3
0.4
0.5
0.6
0.7
0.8
Xm
(c)
Other
Chalk
Paleogene
Frequency
12
10
8
6
4
2
0
2
3
4
5
6
7
k
(b)
Frequency
12
10
8
6
4
2
0
2
3
4
5
6
7
L/W
(d)
Frequency
16
14
12
10
8
6
4
2
0
10
20
30
40
50
60
Misfit (%)

Figure 8

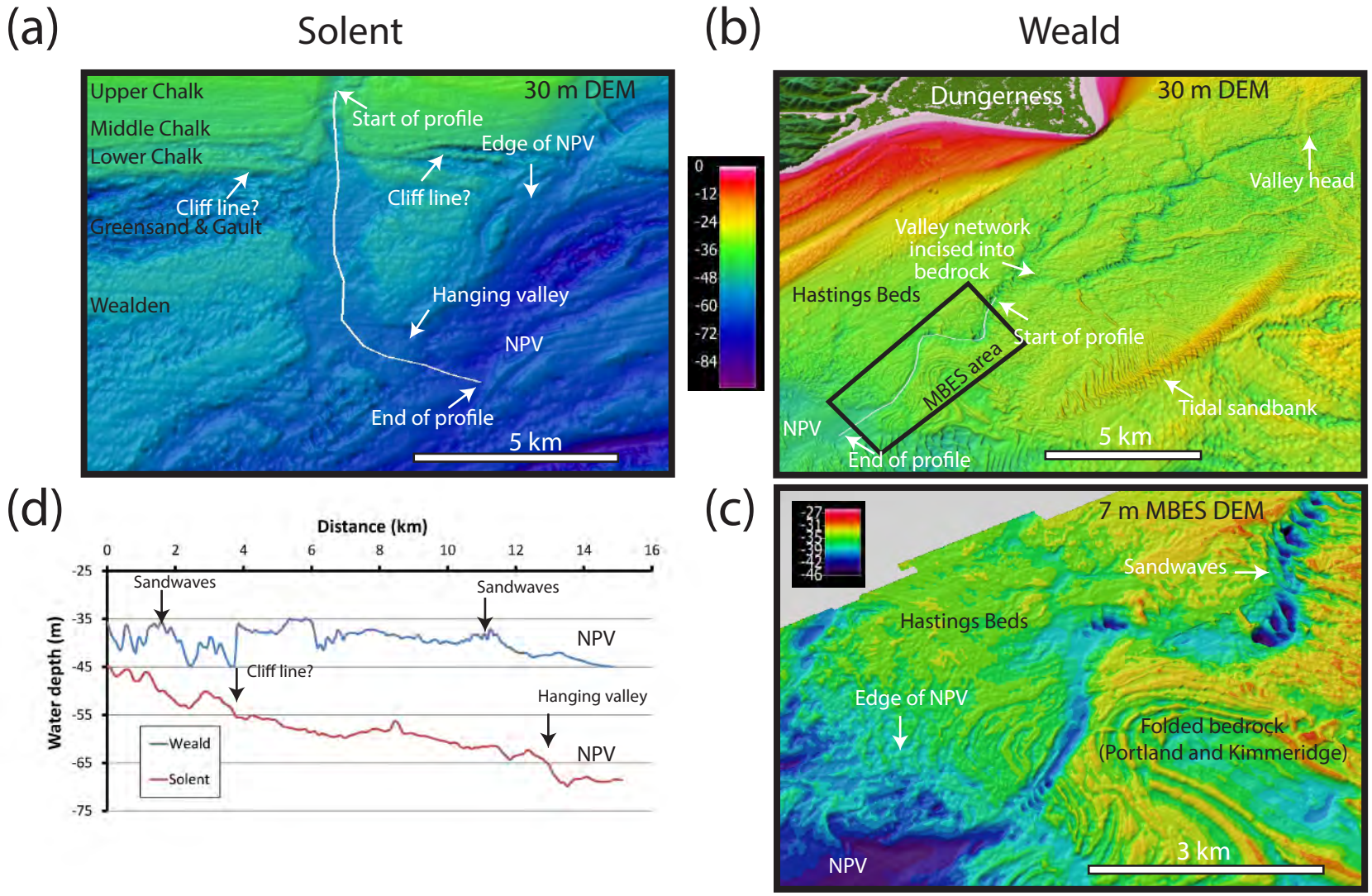
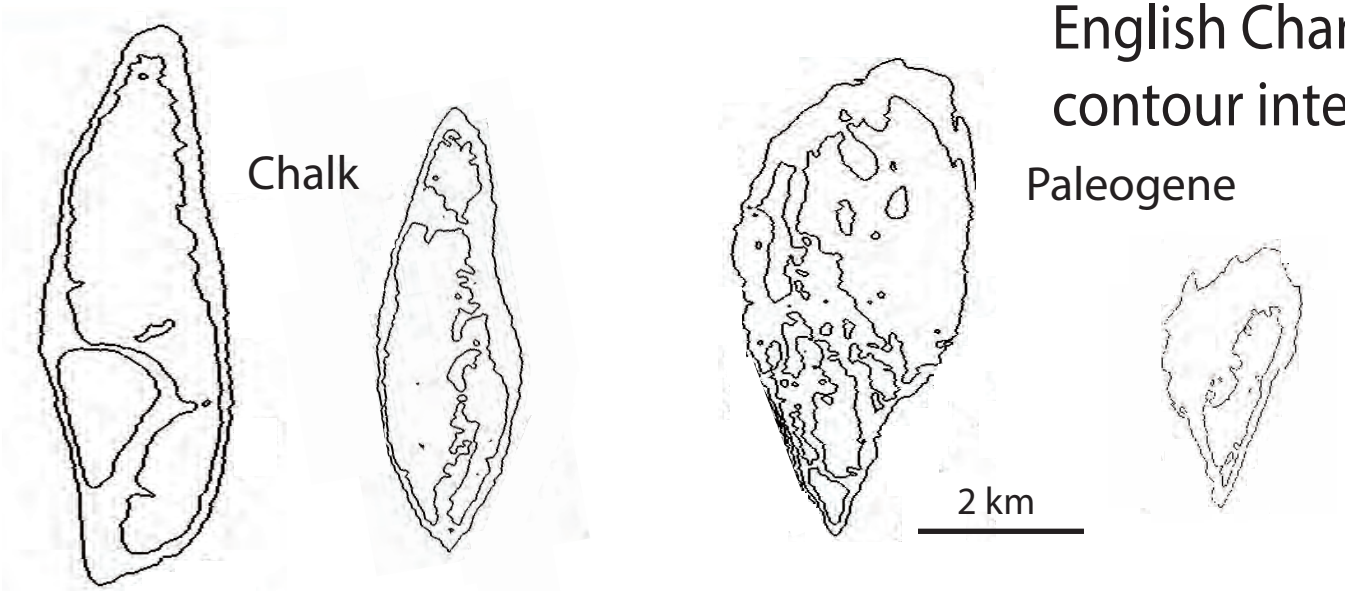

(a)
Solent
Upper Chalk
Middle Chalk
Lower Chalk
Greensand & Gault
Wealden
30 m DEM
Start of profile
Edge of NPV
Cliff line?
Cliff line?
Hanging valley
NPV
End of profile
5 km
0
-12
-24
-36
-48
-60
-72
-84
(b)
Weald
Dungerness
30 m DEM
Valley head
Valley network incised into bedrock
Hastings Beds
Start of profile
MBES area
Tidal sandbank
NPV
End of profile
5 km
(d)
Distance (km)
0
2
4
6
8
10
12
14
16
-25
-35
-45
-55
-65
-75
Water depth (m)
Sandwaves
Sandwaves
NPV
Cliff line?
Hanging valley
NPV
Weald
Solent
(c)
7 m MBES DEM
Sandwaves
Hastings Beds
Edge of NPV
Folded bedrock
(Portland and Kimmeridge)
NPV
3 km

Figure 9


English Channel
contour interval 5 m
Chalk
Paleogene
2 km
Island 26: k=4.9
Island 32: k=4.1
Island 20: k=3.0
Island 22: k=2.6

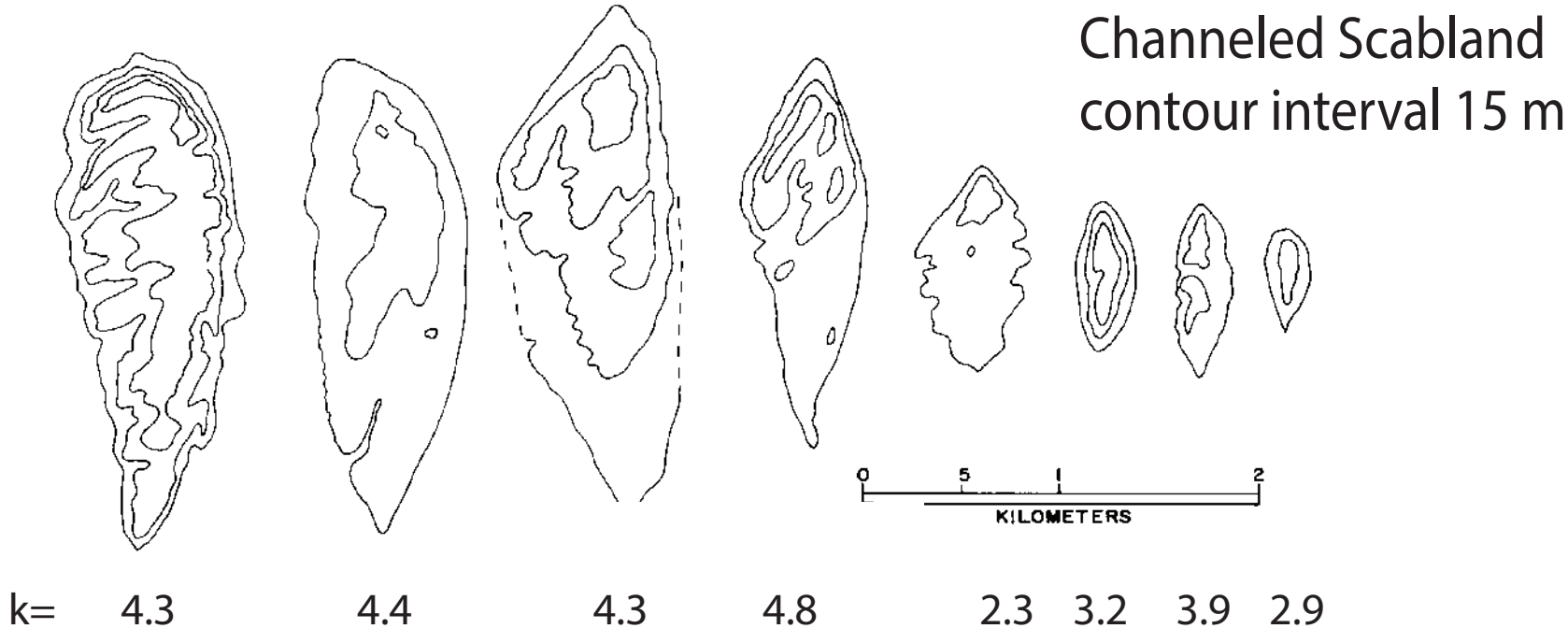
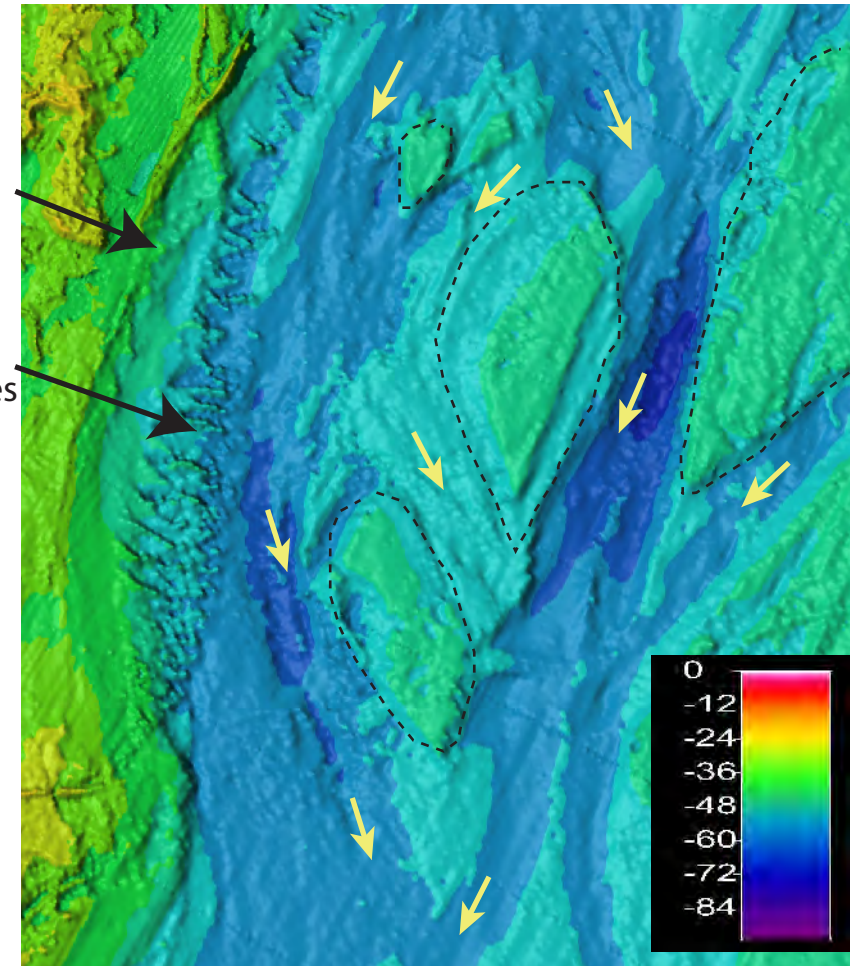

Channeled Scabland
contour interval 15 m
0 5 1 2
KILOMETERS
k= 4.3 4.4 4.3 4.8 2.3 3.2 3.9 2.9

Figure 10a

English Channel



Channeled Scabland

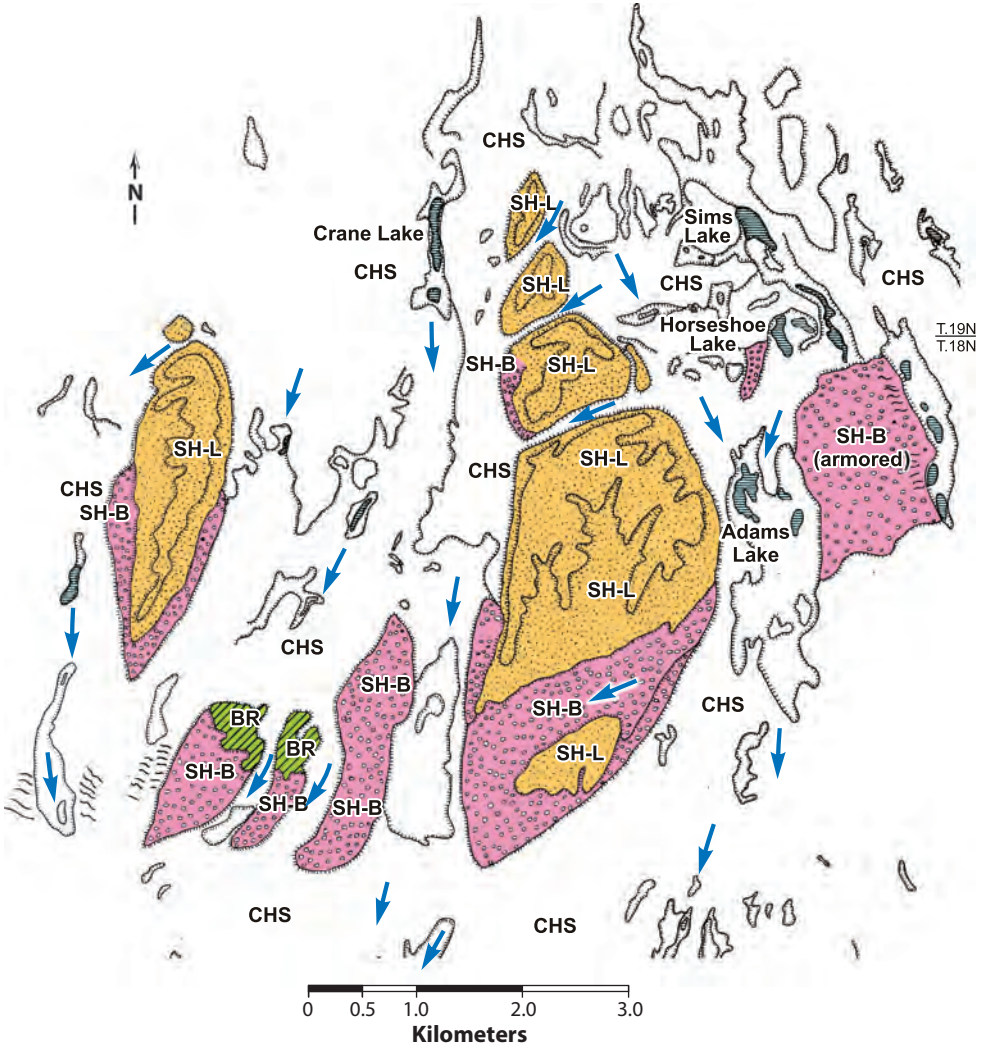


Figure 10b

Table

Epoch	Formation	Sub Unit	Max Age	Max Thickness	Lithology
Paleogene	HAMSTEAD BEDS/ BEMBRIDGE MARLS		Oligocene	80/150 m	Mudstones, thin sands/Limestones and calcareous mudstones.
	BARTON/ BRACKLESHAM/ BAGSHOT BEDS		Eocene	110/200/40 m	Interbedded fine-grained sandstone, siltstone and mudstone with local beds of flint-pebble gravel.
	LONDON CLAY		Eocene	100 m	Fairly homogeneous mudstone.
	READING BEDS		Palaeocene	50 m	Variable - mudstone, sandstone and gravels.
Upper Cretaceous		Upper	Turonian	400 m	White chalk with beds of flint, nodular chalks, hardgrounds and marl seams.
	CHALK	Middle	Cenomanian	70 m	White pure chalk with some flint seams and very shelly beds.
		Lower	Cenomanian	80 m	Grey marly chalk with marl content decreasing upwards. No flint.
Lower Cretaceous	UPPER GREENSAND/ GAULT		Albian	60/50 m	Mudstone with a sandy base.
	LOWER GREENSAND		Aptian	250 m	Medium- and coarse-grained sands and weakly cemented sandstones.
	WEALDEN SERIES	Weald Clay	Hauterivian	300 m	Mainly silty clay and clayey silt, with silts, sands, ironstones and clay ironstones.
		Hastings Beds	Ryazanian	470 m	Interbedded sandstones, siltstones and shales.
Upper Jurassic	PURBECK BEDS		Portlandian	180 m	Interbedded mudstones, limestones and evaporites.
	PORTLAND BEDS		Portlandian	45 m	Upper part predominantly limestone; lower part predominantly argillaceous, dolomitic sandstones/sands.
	KIMMERIDGE CLAY		Kimmeridgian	560 m	Mudstones; thin siltstone and cementstone beds; locally sands and silts.

TABLE 1

Group	Number	Easting	Northing	Area (km2)	Length (km)	Width (km)	Direction (deg)	Xm	L/W	k	Misfit (%)	Bedrock		Illustration	
	1	395179	5658409	2.5	2.8	1.3	75	0.54	2.2	2.5	20	Chalk	Middle Chalk	Fig4b	
1	2	386430	5631731	11.0	7.5	1.9	84	0.31	3.9	4.1	37	Mixed	Hastings Beds/Purbeck/Portland/Kimmeridge	Fig4b	Fig6a
1	3	387971	5619849	10.8	6.5	2.3	68	0.62	2.8	3.0	16	Jurassic	Purbeck/Portland/Kimmeridge	Fig6a	
1	4	376272	5612166	57.2	17.5	4.3	40	0.65	4.1	4.2	31	Mixed	Hastings Beds/Purbeck/Portland/Kimmeridge	Fig4b	Fig6a
2	5	336992	5602060	83.7	20.6	6.1	3	0.44	3.4	4.0	26	Mixed	Chalk/Reading Beds/London Clay		
2	6	333720	5611241	9.3	7.9	1.6	31	0.38	5.1	5.3	34	Mixed	Wealden/Lower Greensand	Fig7a	
2	7	328602	5605266	3.5	4.4	1.1	6	0.39	3.9	4.4	35	Chalk	Upper Chalk		
2	8	328602	5609191	55.6	19.6	3.7	14	0.29	5.3	5.4	45	Mixed	L Greensand/Lower to Upper Chalk	Fig4b	Fig6b
2	9	326350	5606706	9.6	7.9	1.7	22	0.35	4.7	5.1	32	Chalk	Middle to Upper Chalk		
2	10	258236	5603165	5.4	4.3	1.6	8	0.70	2.7	2.6	20	Palaeogene	Reading Beds/London Clay		
2	11	321744	5604303	0.8	2.0	0.6	6	0.55	3.2	3.7	27	Chalk	Upper Chalk		
2	12	319850	5605276	6.3	7.1	1.3	15	0.40	5.3	6.3	39	Chalk	Upper Chalk	Fig4b	
2	13	320199	5601618	2.3	4.1	0.8	-15	0.22	5.3	5.7	50	Palaeogene	London Clay	Fig4b	
2	14	317581	5600982	0.9	1.5	1.0	9	0.52	1.5	1.9	20	Palaeogene	London Clay/Bracklesham Beds		
2	15	312834	5605368	5.0	6.1	1.1	-10	0.72	5.6	5.9	22	Chalk	Upper Chalk	Fig7b	
2	16	308212	5602647	33.6	14.7	3.6	-11	0.48	4.1	5.0	28	Paleogene	London Clay/Bracklesham Beds		
2	17	308863	5607697	3.0	3.6	1.3	25	0.49	2.9	3.5	19	Chalk	Upper Chalk	Fig6b	
2	18	306858	5607433	1.2	2.7	0.6	33	0.39	4.3	4.5	24	Chalk	Upper Chalk		
	19	294289	5606856	5.5	3.9	1.9	1	0.60	2.0	2.2	6	Paleogene	London Clay/Bracklesham Beds	Fig7c	
3	20	258236	5599649	40.0	12.3	5.1	4	0.61	2.4	3.0	16	Paleogene	Bracklesham/Barton Beds	Fig4b	Fig9
3	21	253989	5605781	1.3	1.9	1.0	23	0.69	1.9	2.0	12	Paleogene	Bracklesham/Barton Beds	Fig3	
3	22	252816	5602745	9.9	5.7	1.6	35	0.53	3.7	2.6	28	Paleogene	Bracklesham/Barton Beds	Fig9	
3	23	247592	5600864	5.6	4.5	1.8	52	0.44	2.5	2.8	14	Paleogene	Bracklesham Beds		
3	24	247474	5595904	3.9	4.4	1.1	41	0.57	3.9	3.9	30	Chalk	Upper Chalk	Fig5	
3	25	242046	5593941	6.1	6.8	1.3	47	0.57	5.4	6.0	18	Chalk	Upper Chalk	Fig5	
3	26	236595	5594515	16.5	10.1	2.3	37	0.48	4.5	4.9	34	Chalk	Upper Chalk	Fig5	Fig9
3	27	233031	5590444	1.1	1.5	1.1	35	0.61	1.5	1.7	22	Chalk	Upper Chalk	Fig5	
3	28	230158	5589987	4.7	4.0	1.8	48	0.60	2.2	2.6	19	Chalk	Upper Chalk	Fig4b	Fig5
3	29	226020	5589278	1.2	2.1	0.9	60	0.53	2.2	2.8	18	Chalk	Upper Chalk	Fig5	
3	30	223445	5587733	7.9	4.4	2.6	20	0.53	1.7	2.0	30	Chalk	Lower to Upper Chalk	Fig5	
3	31	224476	5579696	81.0	19.0	6.4	24	0.60	3.0	3.5	19	Lower Cretaceous	Lower Greensand/Gault/Wealden	Fig4b	Fig5
4	32	204079	5565627	15.2	8.9	2.6	18	0.42	3.5	4.1	33	Chalk	Undifferentiated Chalk	Fig5	Fig9
4	33	190568	5568149	2.0	4.2	0.6	4	0.59	6.5	6.8	20	Paleogene	London Clay	Fig5	
4	34	196974	5563344	6.9	4.7	1.9	60	0.51	2.4	2.5	31	Chalk	Undifferentiated Chalk	Fig4b	Fig5
4	35	188867	5558561	116.2	15.1	10.3	50	0.55	1.5	1.5	32	Chalk	Undifferentiated Chalk	Fig4b	Fig5
4	36	178545	5560407	47.4	11.9	5.6	50	0.59	2.1	2.4	23	Chalk	Undifferentiated Chalk	Fig4b	Fig5
							AVERAGE	**0.51**	**3.42**	**3.73**	**26**				
							ST DEV	**0.12**	**1.3**	**1.4**	**9**				

TABLE 2

Area	Reference	Set of islands	n	L/W	$L=aW^b$ a	b	R^2	Komar (1983) factors Xm	k
English Channel	This study	Entire population	36	3.42 (1.3)	3.32	0.96	0.69	0.51 (0.12)	3.73 (1.4)
(Southern North Sea Lake)		Chalk Islands*	18	3.21 (1.3)				0.5 (0.09)	3.5 (1.5)
		Paleogene islands*	9	3.0 (1.5)				0.57 (0.08)	3.2 (1.6)
KNOWN MEGAFLOOD TERRAINS									
Channeled Scablands	Komar, 1984 (data from Baker, 1979)	Entire population	135	3.15 (1.13)	3.01	1.02	0.76	0.65-0.7	2.9-4.3
(Glacial Lake Missoula)									
Northern Great Plains	Kehew & Lord, 1986	Entire population	168	3.39 (1.43)	3.06	0.97	0.73	0.54 (0.15)	3.65 (1.42)
(Glacial Lake Regina/Souris)		Lemniscate only	34	2.88 (0.88)	2.69	0.98	0.76	0.68 (0.1)	3.16 (1.02)
Northern Sweden	Elfstrom & Rossbacher, 1985	Entire population	9	2.50	ng	ng	ng	ng	1.2-4.5
(Baltic Ice Lake)									ave 2.9
Northern Germany	Meinsen et al., 2011	Entire population	127	3.30	ng	ng	ng	ng	ng
(Glacial Lake Weser)									
MODERN RIVERS									
America	Wyrick (2005)	13 rivers	420	4.14	4.31	0.98	0.92	ng	ng
		Lemniscate only	140	3.87	3.86	0.99	0.94	ng	ng
	Komar, 1984	3 rivers	38	4.30 (0.84)	4.01	0.96	0.98	0.65 (0.06)	ng
Global	Holzweber et al., 2014	30 rivers	452	3.57	4.11	1.00	0.96	ng	ng
Australia	Tooth & Nanson, 2000	Marshall River	25	3.25 (0.57)	3.35	0.97	0.86	ng	ng
MARS									
Maja & Kasei Valles	Komar, 1984 (data from Baker, 1979)	Lemniscate only	47	3.25 (1.57)	4.05	0.95	0.72	ng	1.5-12.0 ave 3.8

* excluding islands with lemniscate misfit >35%
values given as mean (St dev)
ng=not given

TABLE 3